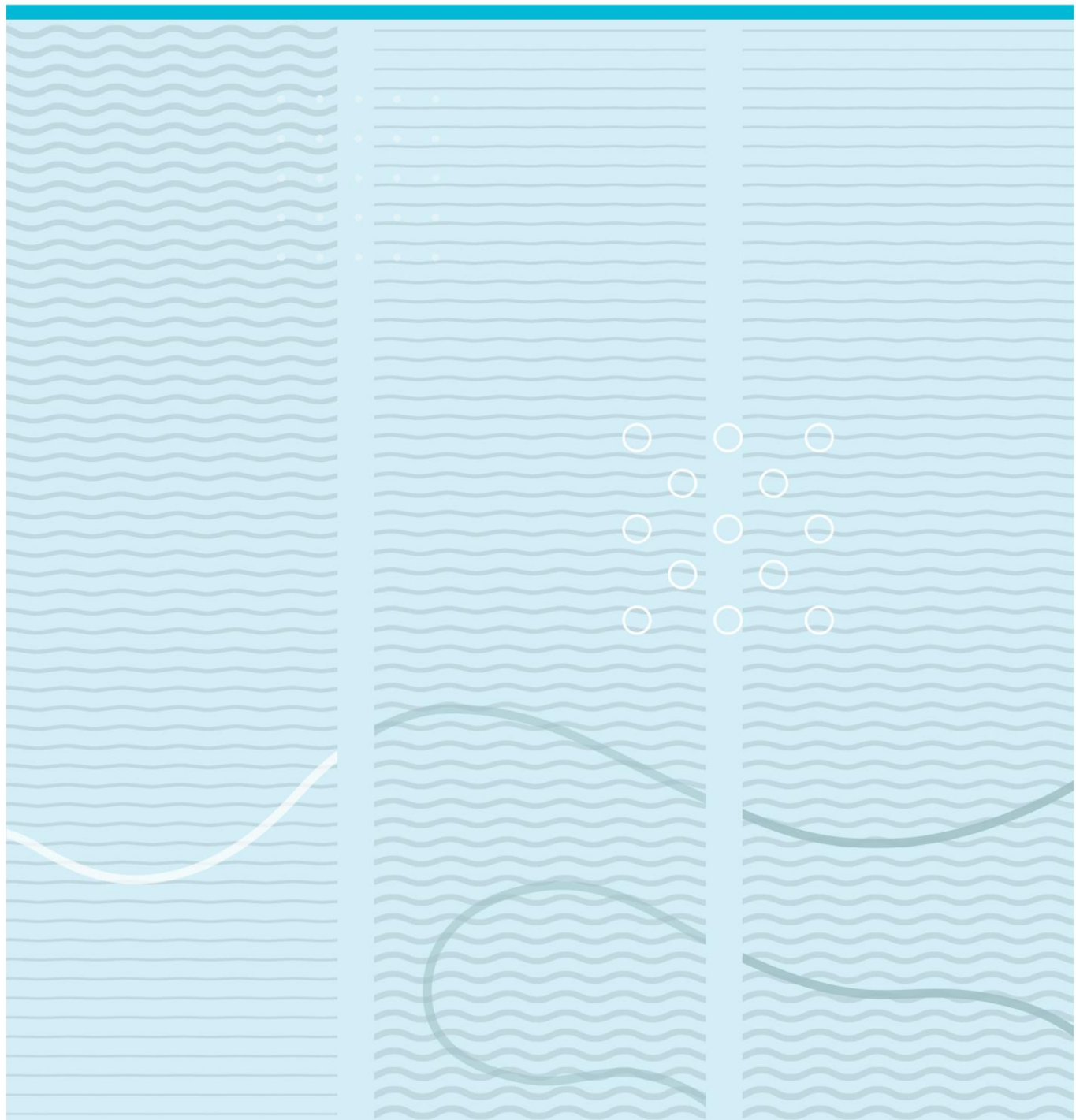


Vyncke Stijn

# Process Tomometric Data Fusion with Multimodal Sensor Suite in Multiphase flow studies



University College of Southeast Norway  
Faculty of Technology  
Institute of Electrical Engineering, IT and Cybernetics  
PO Box 235  
NO-3603 Kongsberg, Norway

<http://www.usn.no>

© 2016 <Vyncke Stijn>

This thesis is worth 30 study points

**University College of Southeast Norway****Faculty of Science, Technology and Marine Technology**  
**M.Sc. Programme**

---

MASTER'S THESIS, COURSE CODE FMH606

Student: &lt;Vyncke Stijn&gt;

Thesis title: &lt;Process Tomometric Data Fusion with Multimodal Sensor Suite in Multiphase flow studies&gt;

Signature: .....

Number of pages: &lt;84&gt;

Keywords: .....

.....

Supervisor: &lt;Saba Mylvaganam&gt; Sign.: .....

2<sup>nd</sup> supervisor: <name> Sign.: .....

Censor: &lt;name&gt; Sign.: .....

External partner: &lt;name&gt; Sign.: .....

Availability: &lt;Open/Secret&gt;

Archive approval (supervisor signature): Sign.: ..... Date : .....

...

**Abstract:**

The objective of the thesis is to propose simple tests on raw electrical measurements, using electrical capacitance tomography in order to assess the prevailing flow regime in the test section. This information regarding the flow patterns is useful in itself in many scientific and technological applications: it can be used in computational fluid dynamics (CFD) for fine-tuning the input parameters, increasing safety on site by providing information about dangerous flow patterns such as slug. In electrical tomography, the reconstruction of an image from the electrical measurements is greatly enhanced when one can postulate what approximately the test area looks like in real time (i.e. flow patterns). By using the raw data coming from the sensor, we avoided the image processing and proposed criteria for different flow patterns. Fang and Cumberbatch have proposed to analyse the eigenvalues of the capacitance data matrix in order to identify core annular or stratified flows. They argue that the analysis of eigenvalues collapses the amount of data to be processed and has the advantage that the analysis is rotationally invariant. Their study has been completely based on numerical simulations of the response of an electrical capacitance tomography (ECT) sensor. Based on their work, we have considered the analysis of eigenvalues of the capacitance matrix but obtained the test criteria based on experimental data, gathered during measurement sessions. We have focused on flow regimes occurring in horizontal pipes. Our tests somewhat differ from Fang and Cumberbatch. One criterion differentiates intermittent flows (plug and slug) from static flows (stratified, wavy and annular) based on the standard deviation of the time series set of the capacitance measurements. The second criterion differentiates annular flows from layered flows (stratified and wavy). For intermittent flows, we have found another criterion using the gamma-ray sensor. A Fast Fourier Transform (FFT) was applied to the time series. This gave us the frequency of plugs and slugs. With this criterion, we can identify intermittent flows.

University College of Southeast Norway accepts no responsibility for results and conclusions presented in this report.

# Abstract

The objective of the thesis is to propose simple tests on raw electrical measurements, using electrical capacitance tomography in order to assess the prevailing flow regime in the test section.

This information regarding the flow patterns is useful in itself in many scientific applications: it can be used in computing fluid dynamics (CFD) for fine-tuning the input parameters, increasing safety on site by providing information about dangerous flow patterns such as slug. In electrical tomography, the reconstruction of an image from the electrical measurements is greatly enhanced when one can postulate what approximately the test area looks like in real time (i.e. flow patterns). By using the raw data coming from the sensor, we avoided the image processing and proposed criteria for different flow patterns.

Fang and Cumberbatch have proposed to analyse the eigenvalues of the capacitance data matrix in order to identify core annular or stratified flows. They argue that the analysis of eigenvalues collapses the amount of data to be processed and has the advantage that the analysis is rotationally invariant. Their study has been completely based on numerical simulations of the response of an electrical capacitance tomography (ECT) sensor.

Based on their work, we have considered the analysis of eigenvalues of the capacitance matrix but obtained the test criteria based on experimental data, gathered during measurement sessions. We have focused on flow regimes occurring in horizontal pipes. Our tests somewhat differ from Fang and Cumberbatch. One criterion differentiates intermittent flows (plug and slug) from static flows (stratified, wavy and annular) based on the standard deviation of the time series set of the capacitance measurements. The second criterion differentiates annular flows from layered flows (stratified and wavy). For intermittent flows, we found another criterion using the gamma-ray sensor. A Fast Fourier Transform (FFT) was applied on the time series. This gave us the frequency of plugs and slug. Due to this criterion, we can identify intermittent flows.

# Contents

<b>1.</b>	<b>Introduction .....</b>	<b>8</b>
<b>2.</b>	<b>Multimodal process tomometry .....</b>	<b>9</b>
2.1.	Introduction .....	9
2.2.	Concept of tomography.....	9
2.3.	Tomographic sensors.....	10
2.3.1.	Electrical capacitance tomography.....	11
2.4.	Gamma-ray densitometry .....	12
<b>3.</b>	<b>Flow regimes in multiphase flow.....</b>	<b>13</b>
3.1.	Introduction .....	13
3.2.	Multiphase flow patterns .....	13
3.2.1.	Flow regime maps.....	15
3.2.2.	Forming mechanisms of different flow regimes .....	15
3.2.3.	Flow pattern classifications .....	16
3.2.4.	Different types of flow patterns.....	17
<b>4.</b>	<b>Experimental set-up of the multiphase flow rig.....</b>	<b>19</b>
4.1.	Multiphase flow facility .....	19
4.2.	Description of the tiltable pipe for two-phase flow.....	20
4.2.1.	Sensors used for flow pattern characterization .....	21
4.2.1.1.	Tomographic sensor .....	21
4.2.1.2.	Gamma-ray sensor.....	22
4.3.	Programs for data logging and analysis.....	23
4.3.1.	Program for data gathering using tomographic system -ECT32v2 .....	23
4.3.2.	Program for data logging and steering of the multiphase rig in LabVIEW ...	23
<b>5.</b>	<b>Data acquisition at different conditions of flow.....</b>	<b>24</b>
<b>6.</b>	<b>Data analysis of the capacitance measurements .....</b>	<b>25</b>
6.1.	Electric capacitance tomographic data .....	25
6.1.1.	Sensor data protocol .....	25
6.1.1.1.	Absolute capacitance file generation .....	25
6.1.1.2.	Normalized capacitance file generation.....	26
6.1.2.	Processing of the ASCII files .....	27
6.2.	The 12x12 capacitance matrix .....	27

6.2.1.	Calculating diagonal term .....	28
6.3.	Compressing the 12x12x6000 matrix.....	29
6.3.1.	Eigenvalues of the capacitance matrix .....	29
6.4.	MATLAB code for data analysis.....	30
6.4.1.	Calibration, multiple inputs and zero matrix building .....	30
6.4.2.	Reading the data, making the matrices and calculating the eigenvalues. ...	31
<b>7.</b>	<b>Characterization of flow regimes .....</b>	<b>33</b>
7.1.	Intermittent flows.....	34
7.1.1.	Criteria for intermittent flows using eigenvalues .....	35
7.1.2.	Criteria for intermittent flows using gamma-ray data.....	35
7.2.	Annular and Wavy/Stratified flows.....	37
7.3.	Success/fail test of the algorithm. ....	40
<b>8.</b>	<b>Flow regime mapping.....</b>	<b>43</b>
8.1.	Data export from Excel to MATLAB .....	43
8.2.	Mapping of flow regimes .....	44
8.2.1.	Mapping all measurements without flow pattern identification.....	44
8.2.2.	Mapping the flow regimes .....	45
<b>9.</b>	<b>Conclusion and future work .....</b>	<b>48</b>
9.1.	Conclusion.....	48
9.2.	Future work.....	50

## **Foreword**

This thesis assumes basic knowledge of MATLAB. This is used in the chapters where the analysis of the data is discussed and the mapping of the results.

I would like to thank Antoine Dupré for his help with this thesis, Fredrik Hansen for his help with performing the experiments and Saba Mylvaganam for his advice, help and positive spirit. In addition, I would like to thank my girlfriend, friends, family in Belgium and my Norwegian family for their support.

<Porsgrunn, Norway/10.06.2016>

<Stijn Vyncke>

# **1. Introduction**

In this thesis, the goal is to propose simple test for identifying certain types of multiphase flow patterns. The knowledge of the type of flow pattern can be useful in many different applications.

One application could be to make operations safer. In pipelines, a flow pattern called slug can occur. A characteristic of a slug is that it has irregular flows. Liquid accumulates in the pipe and in some cases fill the pipe totally, flows through the pipe and eventually the level in the pipe is low again. This happens in a cyclic behavior. One of the results can be that vibrations occur which can cause severe problems for the whole operation. If a simple test can reveal the flow pattern, actions can be taken in order to prevent the potential problems (e.g. damages to equipment of the process, high level of liquid in multiphase flow separators, floods).

After this introduction, in Chapter 2, 3, 4 and 5, the following topics are discussed: tomography, flow regimes in multiphase flow, the experimental set-up used for the experiments and the data acquisition. This will provide the reader with some general knowledge about the topic.

The Chapters 6, 7 and 8 will describe the methods used to analyze the raw capacitance data, the characterization of the flow regimes and the mapping of the flow regimes using the criteria found for the different flow regimes.

## **2. Multimodal process tomometry**

### **2.1. Introduction**

In this chapter, the tomographic measurement system is described. An enumeration is made of the different types of tomographic sensors and the technique for the electrical capacitance tomography (ECT) is illustrated. In addition, a brief description of gamma-ray densitometry is given.

### **2.2. Concept of tomography**

Industrial process flows consists of complex mixtures of different components. These components can occur in different state of matter: gas, liquid and solid. When the process flows are being controlled and monitored, process tomography gives the operators a real-time flow estimation. This gives the operator a tool to monitor and control flow behavior. This is done mostly non-intrusively using process tomographic systems. The data, coming from the tomographic systems, gives valuable data for:

- Visualization
- Monitoring
- Mathematical model verifications
- Computational fluid dynamics

Due to the complexity of the multiphase process flows, there has been development of tomographic systems, which use multiple electrical properties for generating real-time images. Hence the name, multimodal tomographic systems [Marashdeh et al., 2007].

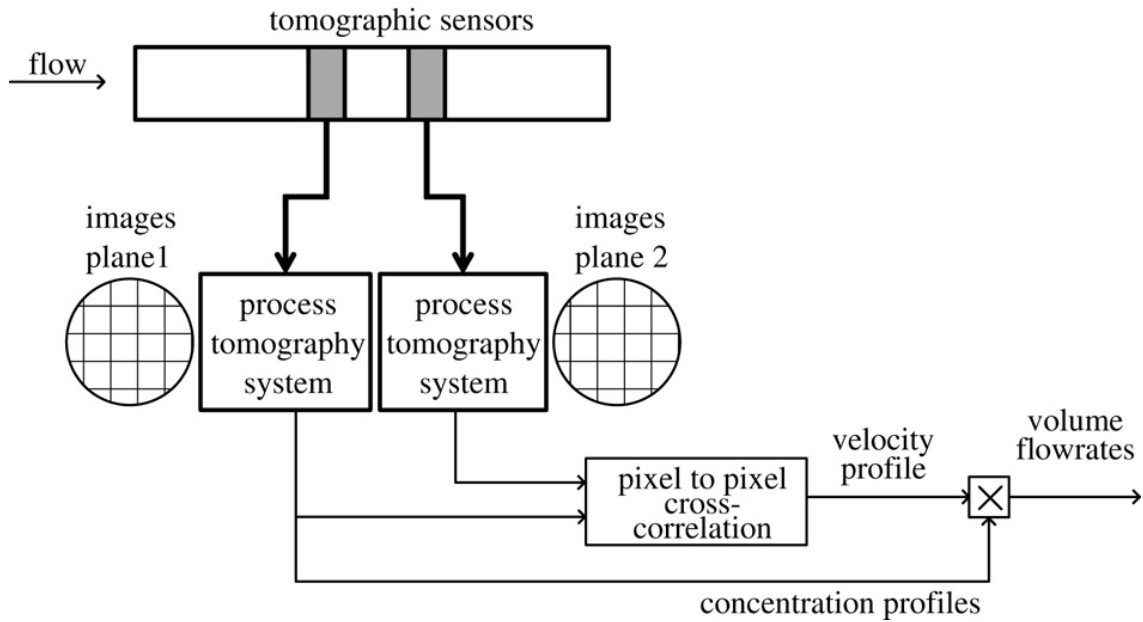


*Figure 2-1: Twin plane tomographic measurement system of a multiphase flow [Ismail et al., 2005].*

### 2.3. Tomographic sensors

There are many different types of tomographic sensors used in process tomography. These include ionizing radiation (e.g. X-ray and gamma-ray), optical, positron emission (PET), magnetic resonance imaging (MRI), acoustic, electrical (capacitive, conductive and inductive) and microwave sensors. Due to the different physics involved, there are some sensors more suited for specific work than others. Each of the sensors has its advantages and disadvantages. The objects or processes under investigation will determine which sensors is the most reliable for that specific purpose.

The tomographic techniques that use electrical properties have been extensively studied.

There are three different type of techniques:

1. Electrical capacitance tomography (ECT)
2. Electromagnetic tomography (EMT)
3. Electrical resistance tomography (ERT)

One main disadvantage emerges with using electrical techniques. The spatial resolution of the image achieved through these techniques is moderate. The reason behind this is the absence of a direct narrow path between the electrodes [Ismail et al., 2005].

### 2.3.1. Electrical capacitance tomography

This technique derives from imaging industrial processes that contain dielectric materials. The ECT sensor will give the same capacitance measurement if the distribution of the dielectric material in the pipe is not changing. Once the distribution changes, the sensor will display different capacitance measurements.

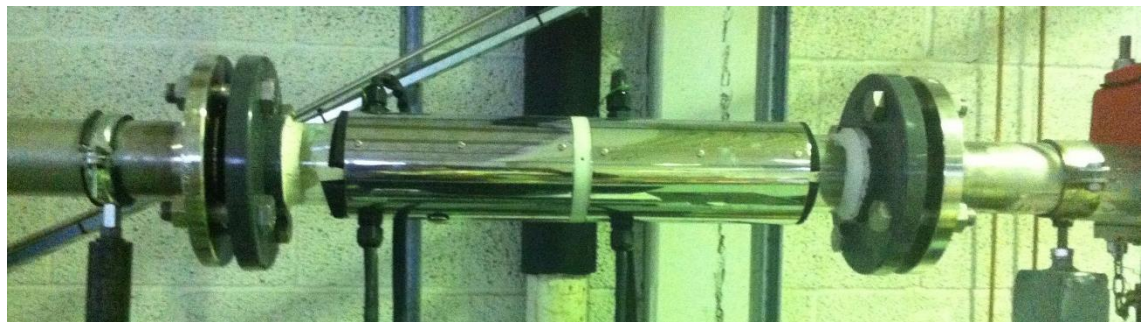


*Figure 2-2: Twin plane ECT sensor mounted in the multiphase flow rig located in the process hall at USN, Porsgrunn.*

The sensor, that takes these capacitance measurements, is a multi-electrode sensor. The most common setup is an ECT sensor with either 8 or 12 electrodes. These electrodes are mounted on the outside of the pipe.

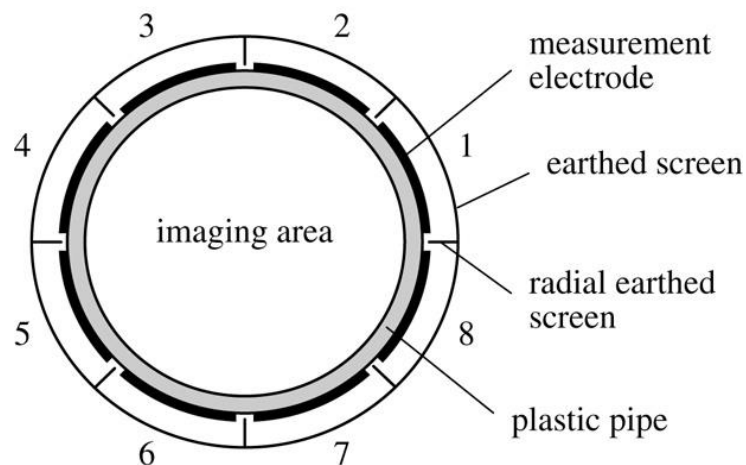


*Figure 2-3: Schematic representation of an 8-electrode ECT-sensor [Ismail et al., 2005]*

There is a non-linear relationship between the measurements and the permittivity distribution. Therefore, when the measurements are used to reconstruct the image, it requires a complicated algorithm. One of the main advantages the ECT-sensor offers is that it is non-intrusive and non-invasive. This means that the flow in the pipe is not disturbed in any way by the sensor.

Other advantages of this technique are no radiation, rapid response and sensor withstands high temperatures and moderate pressure. [Ismail et al., 2005]

## 2.4. Gamma-ray densitometry

With densitometry, the goal is to determine the density of a certain substance, preferably online with nonintrusive sensors. In this study, gamma-rays are sent through the sample and its absorption is used in estimating the density. Here, absorption means any physical interaction between the radiation and the material that reduces the intensity of the incident radiation while penetrating the sample [Schlieper G, 2000].



*Figure 2-4: Gamma-ray sensor mounted in the multiphase flow rig in the process hall.*

### **3. Flow regimes in multiphase flow**

#### **3.1. Introduction**

When dealing with multiphase flows, there are some design difficulties in planning the layout of the pipelines used. Process mechanisms, energy transfer rates, mass and momentum are sensitive towards the geometric distribution or topology of the components within the flow. The understanding of this complex phenomenon is quite challenging. The next chapter discusses the geometric distribution or flow patterns in horizontal pipes. [Brennen C. E, 2005]

#### **3.2. Multiphase flow patterns**

Usually, the identification of the flow patterns happens by visual inspection. Sometimes, the conditions in the pipe make it impossible to do a visual inspection. For instance, if the forces in the pipe are too high, it is possible that a transparent piece of the pipe will become a weak spot and the pipe will break there. This results in the pipe not having any transparent section. To determine which flow patterns is present in the pipe different methods can be used (e.g. gamma-ray densitometry, electrical capacitance tomography). Furthermore, if the identification is done visually, the interpretation can differ from person to person. Very often, the pipe sections are not accessible for process personnel. The characteristics of the different patterns depend on various parameters. One of the parameters is the distribution of fluid phases in space and time. These can change over time and are usually uncontrollable for the operator.

The main goal is to determine how the flow pattern is affected by different parameters such as component volume fluxes, pipe angle and fluid properties (i.e. density, viscosity, surface tension). Many studies have focused on horizontal pipes. Typically, a flow regime map displays the results (Figure 3-1). Different areas of the map present different flow patterns. Where they show up in the map relates to the component flow rates. The flow rates, used in the flow regime map, depend on the author of that map, e.g. volume fluxes, mass fluxes, momentum fluxes or other similar quantities.

The transition region in the flow regime map shown in Figure 3-1 between the different types determine where the flow patterns will change.

The flow regime becomes unstable when it reaches the region. The instability will continue until the formation of another flow pattern.

The range in which two flow regimes changes into each other varies and is hard to predict.

The boundaries are rather a vaguely defined transition zone than a line. Therefore, the multiphase flow regimes change smoothly into each other rather than rapid changes, which would indicate sharp boundaries. The dashed lines in Figure 3-1 display the transition zones [NFOGM, 2005].

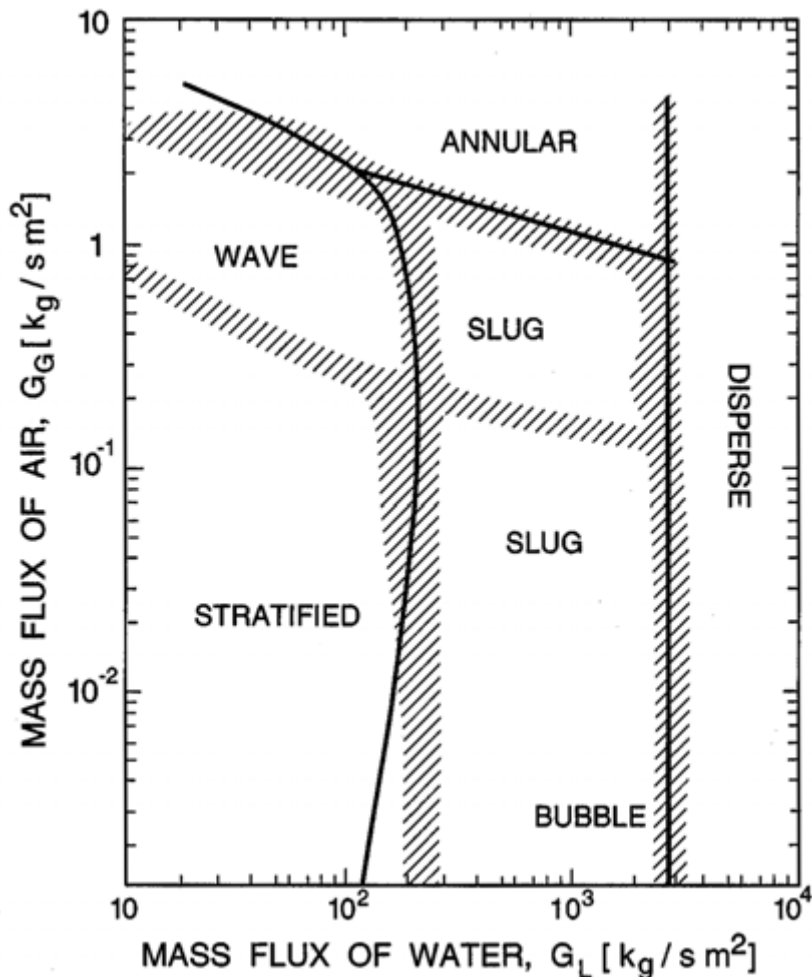


*Figure 3-1: Example of a flow regime map for a horizontal pipe. Hatched regions: observed boundaries zones, continuous lines: theoretically predicted boundaries.*  
[Brennen C. E., 2005]

### 3.2.1. Flow regime maps

A problem that occurs with flow regime maps is that they are only valid for a specific pipe, pressure and a specific multiphase flow (i.e. water-air, water-oil). Once one of these parameters change the flow regime map is no longer the same. The transition zones will move around depending on an increase or decrease of the pipe and pressure or switch of the multiphase flow. [NFOGM, 2005]

### 3.2.2. Forming mechanisms of different flow regimes

The components of the mechanism playing an important role in determining which flow pattern develops in the pipe are [NFOGM, 2005]:

- Transient effects: these effects are the result of changing system boundary conditions; e.g., opening and closing valves.
- Geometry and terrain effects: when the pipe changes geometry or has bends, the flow pattern will be affected. This effect can have severe implications in downstream of sea-lines. The flow regimes generated by these effects can go on for several kilometers; e.g., severe riser slugging.
- If none of the above effects is present, the flow rates, fluid properties, pipe diameter and inclination determine the flow pattern. These flow patterns will occur in horizontal pipes. All the flow patterns combined, formed in these conditions, are called hydrodynamic flow patterns. These patterns are fully developed because they are generated in a horizontal pipe and there is no other external effect that can influence the pattern. In this thesis, the hydrodynamic flow patterns are the ones that will be discussed.

### 3.2.3. Flow pattern classifications

The main characteristic of a multiphase flow pattern is the way in which the liquids and gasses distribution happens along the pipes axial and radial directions. Every flow regime is a member of one three main groups of flow types or a combination of them. The three groups are:

- Dispersed flow: the distribution of the phase is uniform in radial and axial direction; e.g., bubble and mist flow.
- Separated flow: here, the distribution is non-continuous in the radial direction. In the axial direction, the distribution is continuous; e.g., stratified and annular.
- Intermittent flow: non-continuous distribution in the axial direction. Due to this kind of distribution, the flow shows unsteady behavior; e.g., elongated bubble, also known as a plug flow, and slug flow.

There is another way of classifying multiphase flow. This classification uses Gas Volume Fractions (GVF). This method is relevant to multiphase flow metering but irrelevant for this thesis because the aim is to determine the flow pattern, and not the gas volume fractions of the flow. Therefore, the GVF classification is irrelevant [NFOGM, 2005].

### 3.2.4. Different types of flow patterns

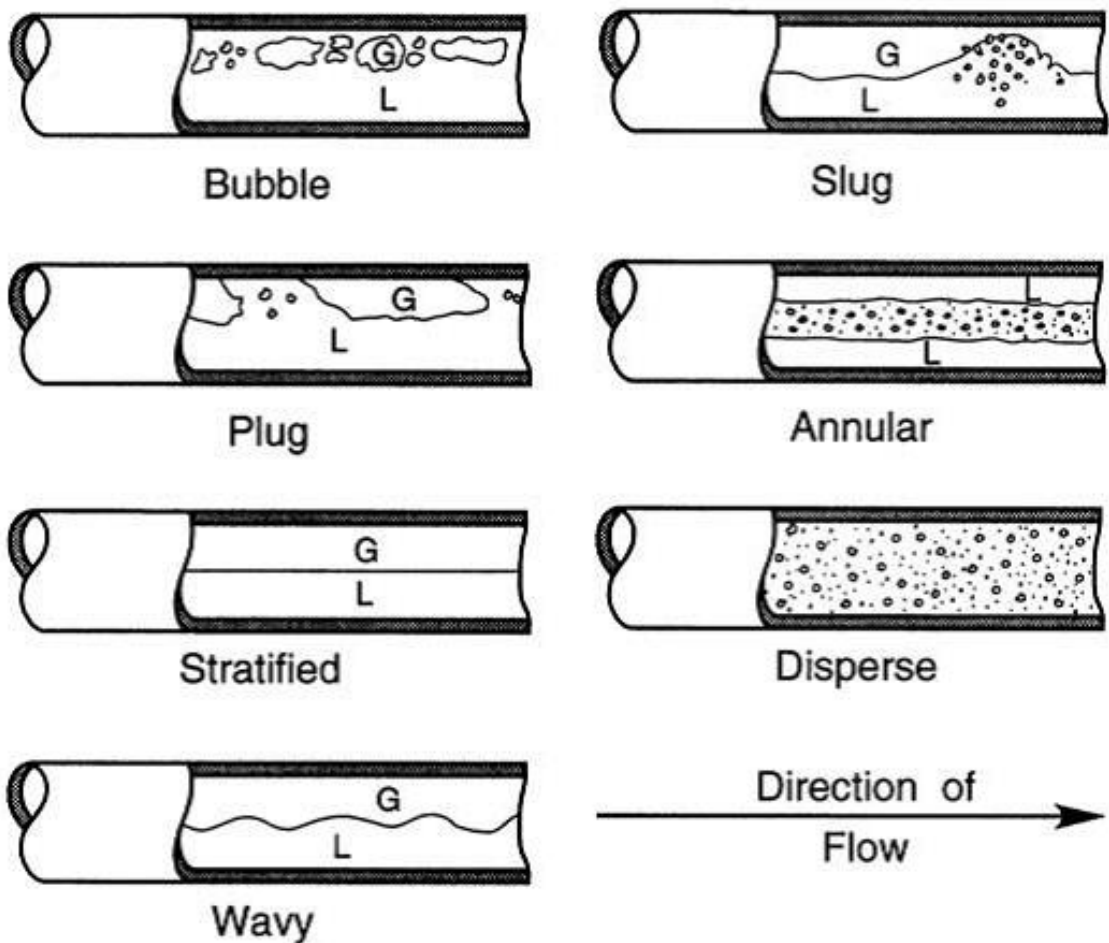


Figure 3-2: Flow regimes for air/water mixture in a horizontal pipe. G is for gaseous phase, L for liquid phase [Brennen C. E., 2005]

Seven different types of flow regimes can occur in horizontal pipes. In Figure 3-2, all different types are sketches. The different flow patterns are listed in Table 3-1.

*Table 3-1: Description of the different flow patterns found in horizontal pipes from our experimental studies and [Brennen C. E., 2005].*

Bubble	The pipe is filled with clear water for the most part. The bubbles will appear in the top of the pipe.
Slug	With slug flow there is an accumulation of water in the pipe that (most of the time) reaches the top of the pipe. There are bubbles in this accumulation.
Plug	Plug is more or less the same as slug. The difference is that in the accumulation, there are very few bubbles and they are not dispersed. .
Annular	The walls of the pipe are covered with a layer of liquid phase. In the middle of the pipe, water is dispersed in the gas phase. This is because centrifugal forces pushed the most dense phase (water) outwards.
Stratified	Liquid phase at the bottom of the pipe, gas phase on top. The interface between the two phases is flat. The reason behind this is that gravity is separating the phases by difference of density.
Disperse	Fine bubbles (liquid phase) are dispersed in the gas phase
Wavy	Same as stratified but interface is wavy.

## 4. Experimental set-up of the multiphase flow rig

### 4.1. Multiphase flow facility

The rig used for experiments consists of many parts. The main components are the horizontal pipe, pumps and separators. A diagram of the rig is displayed in Figure 4-1.

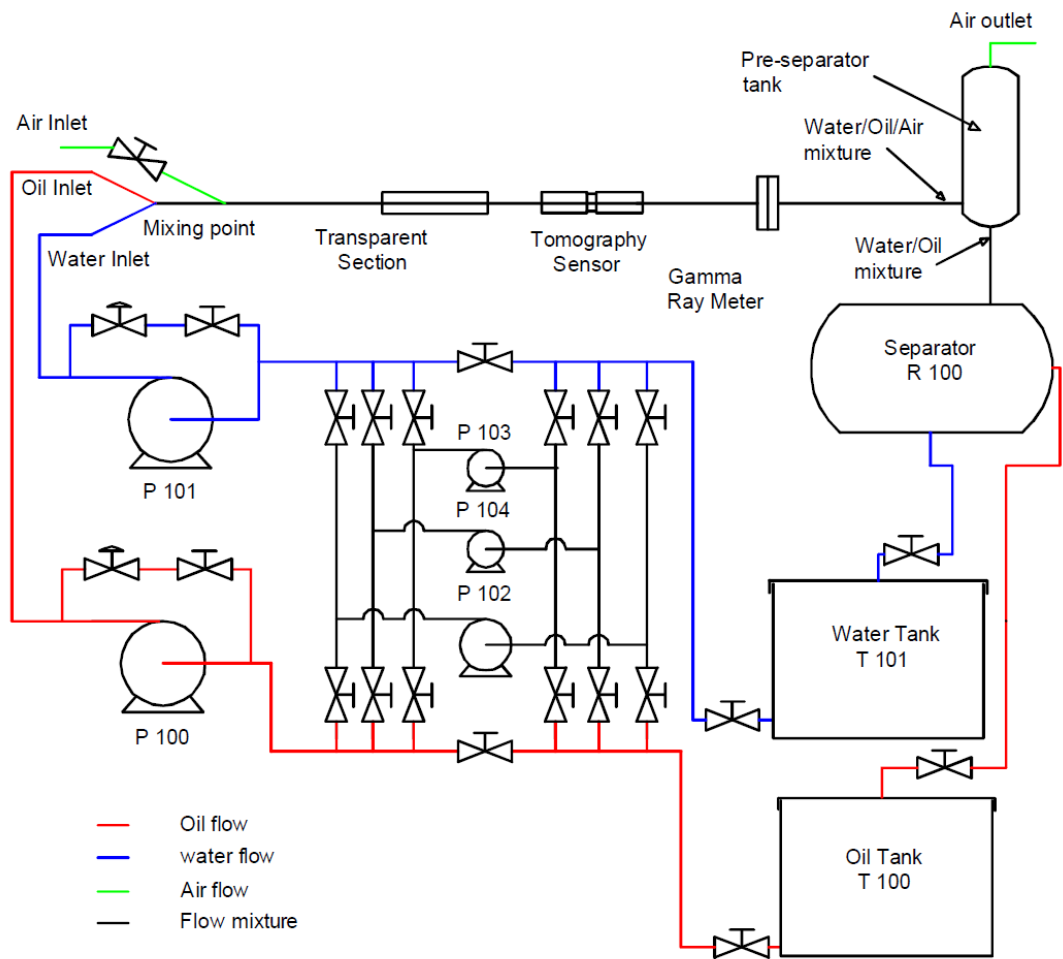


Figure 4-1: Piping and Instrumentation Diagram (PID) of the multiphase flow facility at USN [Pradeep et al., 2014]

The experiments are performed at ambient temperature and room pressure. The two types of liquid that can be used for experiments are distilled water (T101 in Figure 4-1), which might have some contamination, and Exxsol D60 (T100 in Figure 4-1), a transparent mineral oil. These liquids are stored in separate tanks. From there, different pumps transport the liquid to the horizontal pipe. The type of pump used will depend on the volumetric flow rate that is required. The operating ranges of the different pumps are displayed in Table 4-1.

*Table 4-1: Pump specifications for different pumps in the flow loop. The specific pump can be found in the diagram using the pump number. [Hansen et al., 2011]*

Pump number	Type	Flow rate (L/min)	Fluid flow
P100	Positive displacement	80-428	Oil
P101	Positive displacement	80-542	Water
P102	Centrifugal	1.74-13.9	Water/Oil
P103	Positive displacement	0.158-1.5	Water/Oil
P104	Positive displacement	0.455-4.2	Water/Oil

The oil and water enter the pipe at the same spot. The air is injected a little bit further. The air is originated from compressed air tanks. A valve controls the outlet of air. The different flow rates of the liquids and air are measured with Coriolis meters [Pradeep et al., 2014].

## **4.2. Description of the tiltable pipe for two-phase flow**

The two-phase mixture is injected into the 15 m long horizontal pipe in which the flow pattern develops. The liquid mixes with the air at the beginning of the pipe. The angle of the pipe can be adjusted to study the behavior of the flow patterns with different inclinations. The angles of the pipe can be: 10, 6, 5, 3 and 1. The angle can be applied in negative or positive direction.

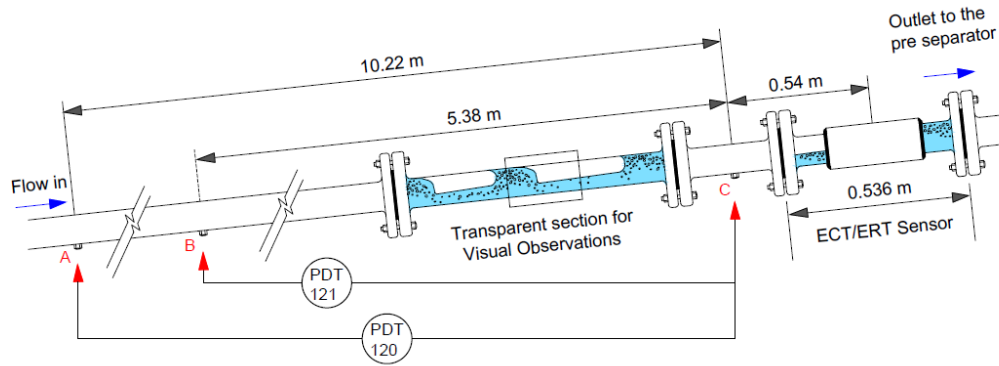


*Figure 4-2: Test section with sensor placements as part of the titled pipe with multiphase flow. Transparent section for high-speed camera base studies and visual observations, multimodal tomographic systems at the far right of the pipe. [Pradeep et al., 2014].*

In the flow loop, there is a Plexiglas transparent section, situated 10 m from the beginning of the pipe. This section is useful for high-speed camera recordings and visual observations of the different flow patterns. If there is a need for visual validation afterward, the high-speed camera will provide the necessary information. A normal recording is also used as validation. The ECT sensor and gamma-ray sensor are installed behind the transparent section [Pradeep et al., 2014]. In Table 4-2, the dimensions of the pipe are given

*Table 4-2: Pipe dimensions in the vicinity of the tomographic systems [Hansen et al., 2011]*

Length	Approx. 15m
Inner Diameter	56 mm
Outer Diameter	65 mm

#### 4.2.1. Sensors used for flow pattern characterization

##### 4.2.1.1. Tomographic sensor

The sensor that is used for gathering the electrical capacitance data is an ECT sensor (Figure 2-2). It is a dual plane sensor with an internal diameter of 56 mm. The sensor has 12 electrodes per plane. It operates at an AC electrical field frequency of 1MHz and acquires 100 frames per second.

The 12 electrodes are each 12.7 mm wide and 85 mm long. They are positioned on the outer diameter of the wall made of dielectric material. [Pradeep et al., 2014]

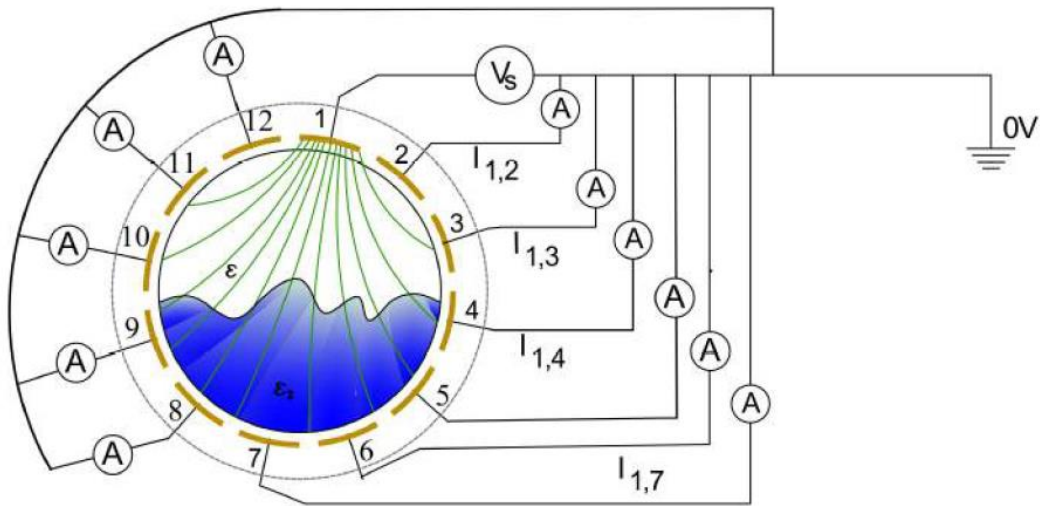


*Figure 4-3: Measurement principle of ECT sensor. Electrode 1 is excited with  $V_s$  and other electrodes are earthed. [Pradeep et al., 2014]*

The capacitance measurements will be taken between two electrodes  $i$  and  $j$ . On electrode  $i$ , the source electrode, an electric potential is applied while electrode  $j$ , the detector electrode, is kept earthed. The resulting electric charge in electrode  $j$  is measured. Every electrode is held at zero potential while one is given an excitation. The one that is given the excitation will change so that every electrode will be the source electrode for one frame. Due to the symmetric nature of the measurements ( $C_{i,j} = C_{j,i}$ ), there are 66 independent measurements in a frame for a 12-electrode sensor. These 66 measurements are mutual capacitance measurements for specific pairs of electrodes [Fang and Cumberbatch, 2004].

#### 4.2.1.2. Gamma-ray sensor

The density is measured with this sensor (Figure 2-4). It is also a non-intrusive sensor. The data gathered from this sensor can also be helpful for determining the flow pattern. The gamma-ray sensor is not suited for distinguishing non-intermittent flows but it helps with distinguishing intermittent against other flows. This data is used to characterize the flow-associated parameters (slug frequency, amplitude...) [Johansen, 2015].

## **4.3. Programs for data logging and analysis**

### **4.3.1. Program for data gathering using tomographic system - ECT32v2**

For gathering data from the ECT sensor, the program ECT32v2 is used. With this program, the data, coming from the sensor, will be stored in binary .bcp files. This type of file needs to be converted into ASCII files for further processing with MATLAB. The ECT32v2 also gives real-time tomographic images of the inside of the pipe during the experiments.

### **4.3.2. Program for data logging and steering of the multiphase rig in LabVIEW**

The multiphase flow loop is controlled with LabVIEW. In the interface, valves and pumps can be operated and the desired flow rates of the phases can be changed here. The measurement taken by the pressure sensors and flow rate sensors will be stored in .txt files. The files are generated synchronously with the ECT data (60 seconds). The flow rates and pressures are logged every second.

The gamma-ray sensors data can be viewed in a LabVIEW interface as well. There is a real-time graphic of the density/time. These measurements will be stored in '.xlsx' files and are used for additional information on the types of flow patterns. The rate at which the measurements are taken is 20Hz.

## 5. Data acquisition at different conditions of flow

In Annex 2, the experiment settings and different types of collectible data are displayed. If the data is gathered for that experiment, the color code is green. Otherwise, it will be red. The data for a particular flow condition can be retrieved by looking for the sample number or the run number.

The flow regime map that is used to predict which flow pattern would be generated is shown in Figure 5-1. Note that this flow regime map is for a horizontal pipe with a diameter of 56mm. The pipe used in the multiphase flow rig is 56mm, so the transition lines will be slightly shifted. This is also used as a guideline to design the experiments sessions. From this map, an indication can be found of the parameters to study certain transitions.

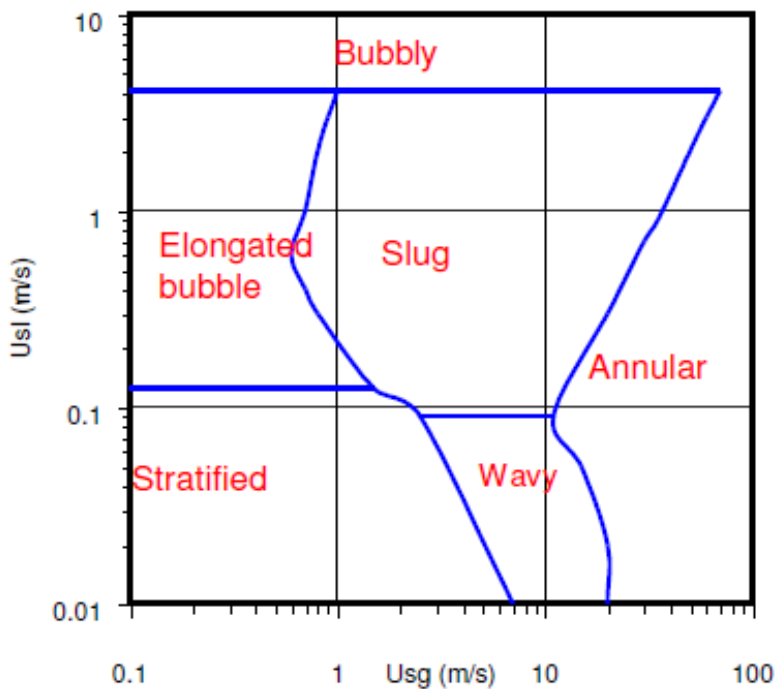


Figure 5-1: Flow regime map for a horizontal 50 mm pipe, air and water 20°C, based on [Mandhane et al., 1974]

The bubbly flow at the top of the flow regime map in Figure 5-1 will not be studied because the rig cannot be operated safely at high water flow rates necessary for this.

## 6. Data analysis of the capacitance measurements

Further analysis is done after all the data is gathered. In the next paragraphs, the analysis of the raw data is explained. The analysis uses the programs ECT32v2 and MATLAB.

### 6.1. Electric capacitance tomographic data

#### 6.1.1. Sensor data protocol

During the experiments, the data gathered by the ECT sensor is saved in .bcp files. These files need to be converted with the ECT32v2 software. With this software, ASCII files can be generated and these files will be used for further analysis. There are two different type of ASCII files: absolute capacitance files ('.aac') and normalized capacitance files ('.anc'). In the latter, the capacitances are normalized with the calibration measurements of reference media (pipe full of water and pipe full of air). Two models can be used for this normalization: the series or the parallel model. In this thesis, the parallel normalization model is used. The effect of the geometric setup of the sensor is expected to be reduced by these normalizations [Fang and Cumberbatch, 2005] [Marashdeh et al., 2007].

##### 6.1.1.1. *Absolute capacitance file generation*

In Figure 6-1, the interface for generating ASCII files is shown. Some parameters need to be changed every time other files are generated:

1. In the Data sources box the .bcp files that will be converted need to be selected as the Capacitance file. Browse to the location of the file. Also, select the calibration file air\_water60l.cal in the Calibration box.
2. Next, select the name and the place of the output file in the Output box.
3. Select the Absolute Capacitance radio button in the Converted data type box. In this box, select the desired plane: Plane 1 or Plane 2.
4. Disabled the Include File Comments.
5. If all of the previous steps are done, click Save and the ASCII file will be generated.

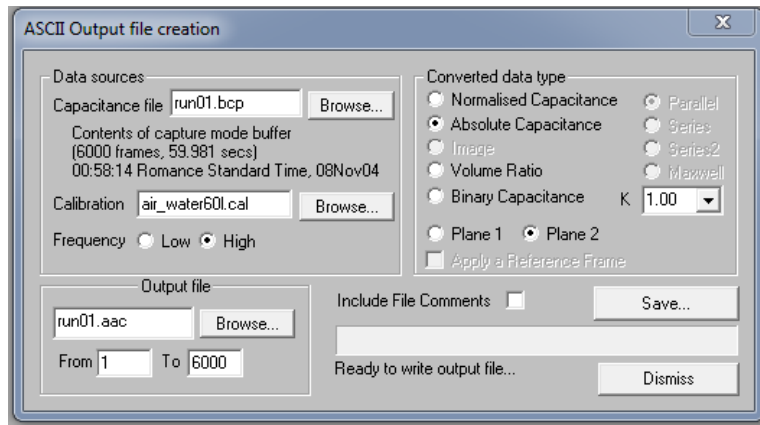


*Figure 6-1: Screen capture from ASCII output ‘.aac’ file generation*

#### 6.1.1.2. Normalized capacitance file generation

In Figure 6-2, the interface for generating ‘.anc’ files is shown. The steps to generate the files are almost similar for ‘.aac’ files (See 6.1.1.1). The differences are:

- The calibration file in the Data sources box must not be selected.
- The radio button for Normalized Capacitance in the Converted data type box needs to be selected.

After these two steps, the ‘.anc’ files can be generated the same ways as ‘.aac’ files are generated.

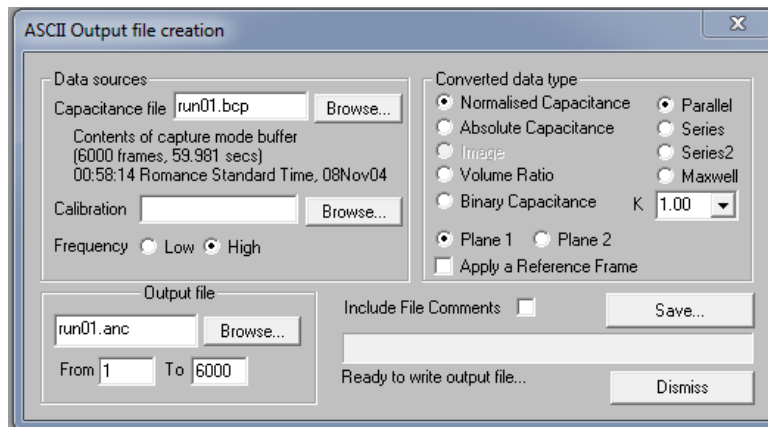


*Figure 6-2: Screen capture of ASCII output ‘.anc’ file generation*

### 6.1.2. Processing of the ASCII files

The generated ASCII files need to be processed. These files contain 6000 tomographic data sets that are collected over a period of 60 seconds. This means that the ECT sensor acquires 100 frames per second. One set of data consists of 66 mutual capacitance measurements (see 4.2.1.1). The totality of these sets of tomographic data will be called a time series.

## 6.2. The 12x12 capacitance matrix

Each frame of the time series that is acquired by the ECT sensor will be converted to a 12x12 matrix for further processing.

*Table 6-1: Normalized capacitance data from the second plane of the ECT sensor run 001.*

Electrode	1	2	3	4	5	6	7	8	9	10	11	12
12	1.056	1.069	1.016	1.080	1.159	1.045	1.017	1.026	1.040	1.041	1.256	
11	1.090	1.010	1.066	1.147	1.033	1.004	1.010	1.022	1.022	1.046		
10	1.071	1.110	1.187	1.067	1.033	1.039	1.051	1.048	1.073			
9	1.098	1.153	1.028	0.996	1.000	1.009	1.008	1.029				
8	1.355	1.098	1.058	1.055	1.064	1.058	1.083					
7	1.347	1.160	1.153	1.154	1.152	1.171						
6	1.077	1.050	1.051	1.047	1.063							
5	1.041	1.031	1.022	1.036								
4	1.064	1.034	1.047									
3	1.077	1.062										
2	1.100											
1												

The data in Table 6-1 will be received from the ASCII-files after generating them. This is only one frame. The total files contains 6000 of these data sets.

The first step in the conversion is to mirror the values along the diagonal term. This is possible because the capacitance measurements are symmetric, meaning that the capacitance measurement between electrode 1 and 12 is the same as the capacitance measurement between 12 and 1. The mirroring is done by a MATLAB code (Annex 3) and is discussed later in this chapter.

*Table 6-2: Normalized capacitance data from run001. The initial data is mirrored around the diagonal term.*

Electrode	1	2	3	4	5	6	7	8	9	10	11	12
<b>12</b>	1.056	1.069	1.016	1.080	1.159	1.045	1.017	1.026	1.040	1.041	1.256	
<b>11</b>	1.090	1.010	1.066	1.147	1.033	1.004	1.010	1.022	1.022	1.046		1.256
<b>10</b>	1.071	1.110	1.187	1.067	1.033	1.039	1.051	1.048	1.073		1.046	1.041
<b>9</b>	1.098	1.153	1.028	0.996	1.000	1.009	1.008	1.029		1.073	1.022	1.040
<b>8</b>	1.355	1.098	1.058	1.055	1.064	1.058	1.083		1.029	1.048	1.022	1.026
<b>7</b>	1.347	1.160	1.153	1.154	1.152	1.171		1.083	1.008	1.051	1.010	1.017
<b>6</b>	1.077	1.050	1.051	1.047	1.063		1.171	1.058	1.009	1.039	1.004	1.045
<b>5</b>	1.041	1.031	1.022	1.036		1.063	1.152	1.064	1.000	1.033	1.033	1.159
<b>4</b>	1.064	1.034	1.047		1.036	1.047	1.154	1.055	0.996	1.067	1.147	1.080
<b>3</b>	1.077	1.062		1.047	1.022	1.051	1.153	1.058	1.028	1.187	1.066	1.016
<b>2</b>	1.100		1.062	1.034	1.031	1.050	1.160	1.098	1.153	1.110	1.010	1.069
<b>1</b>		1.100	1.077	1.064	1.041	1.077	1.347	1.355	1.098	1.071	1.090	1.056

The capacitance data is mirrored around the diagonal term. This results in a 12x12 matrix with the diagonal term empty. This diagonal term needs to be calculated.

### 6.2.1. Calculating diagonal term

The diagonal term represents the self- capacitance of the electrode that is excited at that point in time. Self-capacitance is the amount of electric charge that must be added to an isolated conductor to raise its electric potential by one unit. This characteristic needs to be calculated for each electrode and is done with formula (6-1).

$$C_{i,i} = - \sum_{j \neq i} C_{i,j} \quad (6-1)$$

The sum of all non-diagonal terms on each line is taken. The diagonal term will be calculated using MATLAB. Then, the matrix will be calibrated using the calibration vectors of water and air. After the calculation, the capacitance matrix C is complete and will have the following form:

$$C = \begin{pmatrix} C_{1,1} & \cdots & C_{1,12} \\ \vdots & \ddots & \vdots \\ C_{12,1} & \cdots & C_{12,12} \end{pmatrix} \quad (6-2)$$

This is described by [Fang and Cumberbatch, 2005].

### 6.3. Compressing the 12x12x6000 matrix

The matrix calculated in 6.2 is a matrix for one frame. In the time series, there are 6000 frames and that results in 6000 matrices. This makes that the time series consist of a 12x12x6000 matrix. This series is represented by formula (6-3) where N = 6000.

$$C = \begin{pmatrix} C_{1,1}[n] & \cdots & C_{1,12}[n] \\ \vdots & \ddots & \vdots \\ C_{12,1}[n] & \cdots & C_{12,12}[n] \end{pmatrix}, n = 1, 2, \dots, N \quad (6-3)$$

The matrix needs to be condensed for further analysis. This is done by calculating the mean (6-4) and standard deviation (SD) (6-5) capacitance matrices.

$$C_{mean} = \begin{pmatrix} mean(C_{1,1}[n]) & \cdots & mean(C_{1,12}[n]) \\ \vdots & \ddots & \vdots \\ mean(C_{12,1}[n]) & \cdots & mean(C_{12,12}[n]) \end{pmatrix} \quad (6-4)$$

$$C_{SD} = \begin{pmatrix} SD(C_{1,1}[n]) & \cdots & SD(C_{1,12}[n]) \\ \vdots & \ddots & \vdots \\ SD(C_{12,1}[n]) & \cdots & SD(C_{12,12}[n]) \end{pmatrix} \quad (6-5)$$

The mean and the standard deviation operators are calculated using respectively formulas (6-6) and (6-7).

$$mean(x[n]) = \frac{1}{N} * \sum_{n=1}^N x[n] \quad (6-6)$$

$$SD(x[n]) = \sqrt{\frac{1}{N} * \sum_{n=1}^N (x[n] - mean(x[n]))^2} \quad (6-7)$$

#### 6.3.1. Eigenvalues of the capacitance matrix

Next, the eigenvalues are calculated. The eigenvalues of the mean and standard deviation matrices are worked out using MATLAB. The eigenvalues are represented in a 12-element array. The algorithm, to see which flow pattern is present in the pipe, will be applied on the eigenvalues of the mean and standard deviation matrices.

The eigenvalues that will be calculated from these matrices will be rotationally invariant. That means that the sensors can be rotated without changing the eigenvalues. [Fang and Cumberbatch, 2005]

With this analysis procedure, a 12x12x6000 matrix is condensed into two 12-element arrays: eigenvalues of mean matrix and eigenvalues of standard deviation matrix. The eigenvalues will be used for characterizing the flow regimes.

## 6.4. MATLAB code for data analysis

The calculations, described in the previous paragraphs of this chapter, are done with the MATLAB code ECTMeasurementAnalysis (Annex 3). This code can process multiple '.anc' and '.aac' files in one run.

### 6.4.1. Calibration, multiple inputs and zero matrix building

In the first part of the code, two calibration vectors are shown. Before executing the code, the right calibration vector must be 'uncommented'. This depends on the type of ASCII file used. If the files are '.anc' files, the normalized calibration vector needs to be used. These lines of code can be found in Annex 3.

After this, the multiple files directory will be used. This will locate all the files with the correct file type. This type of file needs to be changed the type of file that will be used. It needs to be the same as the calibration vector file type. Otherwise, errors will occur.

```
number_of_electrode=12;
%%% Multiple input
files = dir('*.anc');
%%% Eigenvalues_SD matrix
Eigenvalues_SD_matrix=zeros(length(files),number_of_electrode);
%%% Eigenvalues_mean matrix
Eigenvalues_mean_matrix=zeros(length(files),number_of_electrode);
```

*Figure 6-3: Multiple files directory load and building of the eigenvalue matrices for all the eigenvalue vectors of the different runs*

Two zero matrices are created in Figure 6-3. The number of columns and rows will depend on the number of electrodes and the number of files that will be processed. Therefore, the number of electrodes used in the specific sensor must be known. The experiments in this thesis are all done with a sensor consisting of 12 electrodes.

#### 6.4.2. Reading the data, making the matrices and calculating the eigenvalues.

The data from the ASCII files are imported into MATLAB using the textscan command. For the full code, see Annex 3. All of the 6000 capacitance measurements are combined in a 66000x11 matrix. The measurements, as shown in Table 6-1, have a triangular form. In the 66000x11, every element without a value will be assigned with [NaN] so that every element exists.

*Table 6-3: Two sets of the 6000 capacitance data processed by the MATLAB code. This is a part of the 66000x11 matrix, called matrix1 in the MATLAB code.*

0,607	-0,025	0,03	0,009	-0,004	0,012	0,014	0,03	0,012	0,072	1,351
0,465	0,02	0,022	-0,015	-0,016	0,02	0	-0,027	0,011	0,026	NaN
0,449	-0,012	0,007	-0,027	-0,008	0,017	-0,015	0,027	0,009	NaN	NaN
0,415	0,009	0,037	-0,031	0,055	0,011	-0,017	-0,019	NaN	NaN	NaN
0,674	0,014	-0,034	0,044	0,002	0,034	-0,031	NaN	NaN	NaN	NaN
0,717	-0,005	0,001	0,023	-0,013	-0,013	NaN	NaN	NaN	NaN	NaN
0,73	0,049	0,068	0,005	-0,024	NaN	NaN	NaN	NaN	NaN	NaN
1,346	0,992	0,579	0,091	NaN	NaN	NaN	NaN	NaN	NaN	NaN
1,368	1,356	0,341	NaN	NaN	NaN	NaN	NaN	NaN	NaN	NaN
1,347	0,55	NaN	NaN	NaN	NaN	NaN	NaN	NaN	NaN	NaN
1,339	NaN	NaN	NaN	NaN						
0,608	-0,025	0,03	0,009	-0,004	0,012	0,018	0,037	0,022	0,079	1,351
0,464	0,02	0,022	-0,015	-0,016	0,02	0,001	-0,025	0,012	0,024	NaN
0,45	-0,012	0,007	-0,027	-0,008	0,018	-0,014	0,028	0,007	NaN	NaN
0,416	0,009	0,037	-0,031	0,056	0,013	-0,016	-0,021	NaN	NaN	NaN
0,682	0,014	-0,034	0,046	0,003	0,036	-0,032	NaN	NaN	NaN	NaN
0,721	-0,006	0,003	0,025	-0,01	-0,013	NaN	NaN	NaN	NaN	NaN
0,725	0,062	0,077	0,014	-0,021	NaN	NaN	NaN	NaN	NaN	NaN
1,346	1,126	0,71	0,165	NaN	NaN	NaN	NaN	NaN	NaN	NaN
1,368	1,356	0,535	NaN	NaN	NaN	NaN	NaN	NaN	NaN	NaN
1,347	0,807	NaN	NaN	NaN	NaN	NaN	NaN	NaN	NaN	NaN
1,339	NaN	NaN	NaN	NaN						

The matrix generated by the MATLAB code is called matrix1.

The next step is to convert the 66000x11 matrix into the 12x12x6000 matrix. In the first line of code, shown in Figure 6-4, the zero matrix is created.

```

matrix=zeros(12,12,N);
for i=[1:12]
    for j=[i+1:12]
        matrix(i,j,:)=matrix1(i:11:i+(N-1)*11,j-i);
        matrix(j,i,:)=matrix(i,j,:);
    end
end
for k=[1:N]
    matrix(:,:,k)=matrix(:,:,k)-diag(sum(matrix(:,:,k),2));      %diagonal term
    matrix(:,:,k)=(matrix(:,:,k)-calibration_air)./(calibration_water-calibration_air);  %calibration
end

```

*Figure 6-4: Generation of 12x12x6000 matrix including the calculation of the diagonal term and the calibration*

In the first part of the code, the capacitance data is mirrored around the diagonal term. The diagonal term is calculated in the second half of the code (see %diagonal term in Figure 6-4) and after that is done, the calibration is applied. Then the 12x12x6000 matrix is complete.

```

matrix_mean=mean(matrix,3);
eigenvalues_mean=transpose(eig(matrix_mean));
matrix_SD=std(matrix,0,3);
eigenvalues_SD=transpose(eig(matrix_SD));

Eigenvalues_SD_matrix(i_files,:)=eigenvalues_SD;
Eigenvalues_mean_matrix(i_files,:)=eigenvalues_mean;
Eigenvalues_CopyMeanRE = horzcat(Eigenvalues_mean_matrix, Eigenvalues_SD_matrix); %copy excel

```

*Figure 6-5: Calculating the mean matrix, standard deviation matrix and their eigenvalues. These values will be written into the zero matrices created in the first part of the code (6.4.1)*

The mean matrix, matrix\_mean, and the standard deviation matrix, matrix\_SD, are calculated using the 12x12x6000 matrix. This results in 12x12 matrices. From these matrices, the eigenvalues are calculated and transposed. Now the eigenvalues are written in the zero matrices, Eigenvalues\_mean\_matrix and Eigenvalues\_SD\_matrix. In the last line of the code, the two matrices are put beside each other so that on one line of the matrix the mean eigenvalues and the standard deviation values are displayed for one run.

This calculation will repeat until every file in a specific folder is done. Then the matrix Eigenvalues\_CopyMeanRE contains all the eigenvalues of the mean and standard deviation matrix of every run. This matrix will be copied to Excel for further analyzing.

## 7. Characterization of flow regimes

The eigenvalues that are calculated will be used for the characterization of the different flow regimes. The eigenvalues are copied from MATLAB into an Excel sheet (see Annex 4). This is more convenient to make different plots and give the values a color code. In the next paragraphs, the algorithm used to determine the flow pattern is discussed. The criteria are found by trial and error. First, we attempt to identify a significant parameter for a given type of flow pattern. When the parameter is found, the threshold would be fine-tuned until the best results are obtained, Figure 7-1.

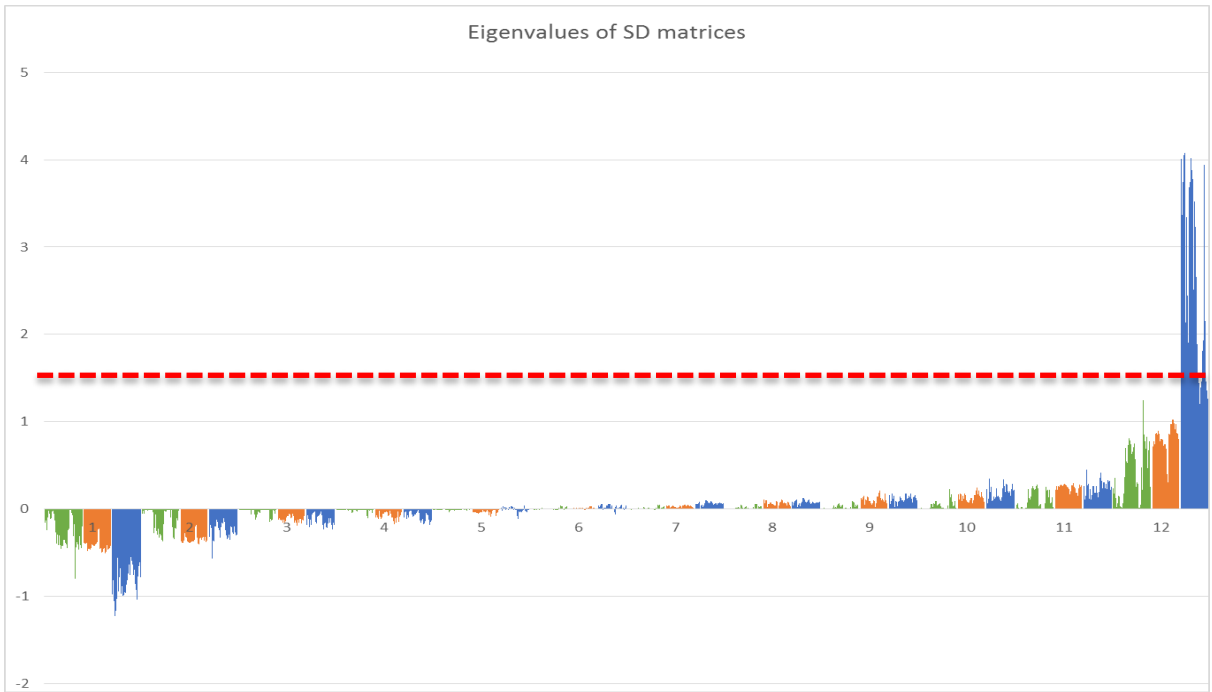


*Figure 7-1: Eigenvalue graph of standard deviation matrices. Green represents stratified and wavy flows, orange represents annular flow and blue represents slug and plug flows.*

The 12<sup>th</sup> eigenvalues of the standard deviation matrices varies significantly for different types of flow patterns. The blue lines, intermittent flows, have a much higher value than the other ones. This parameter was then chosen to identify the intermittent flows and the threshold was set at 1.5 (see dashed line in Figure 7-1). Afterward, the threshold was fine-tuned to have better results.

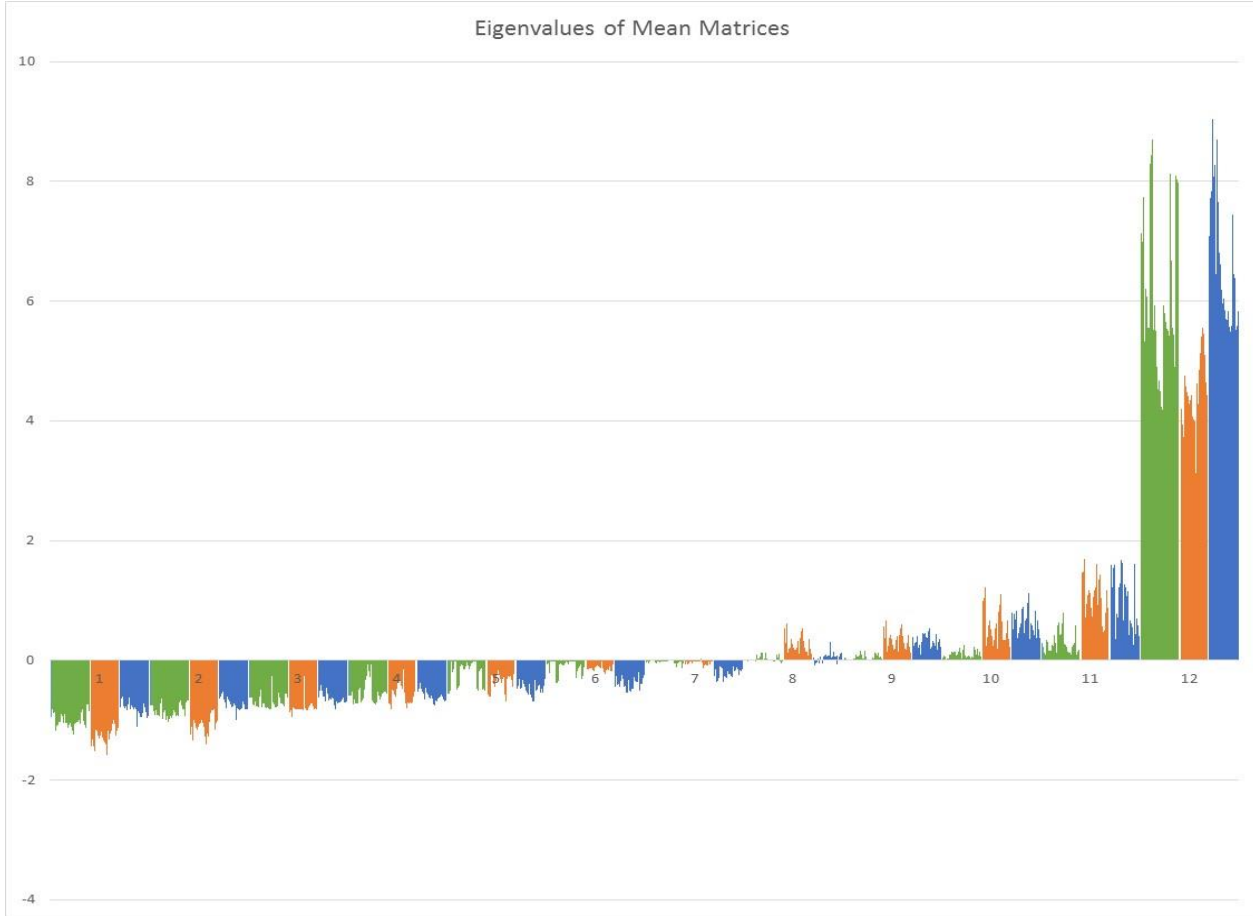


*Figure 7-2: Eigenvalue graph of mean matrices. Green represents stratified and wavy flows, orange represents annular flow and blue represents slug and plug flows.*

## 7.1. Intermittent flows

The first criterion used in the algorithm is to determine if the flow is an intermittent flow. This is a group of flow patterns that include plug and slug flows (see 3.2.3). The algorithm uses the 12<sup>th</sup> eigenvalue form the  $C_{sd}$  matrix. In addition, the gamma-ray sensor can be used to determine this type of flows.

### 7.1.1. Criteria for intermittent flows using eigenvalues

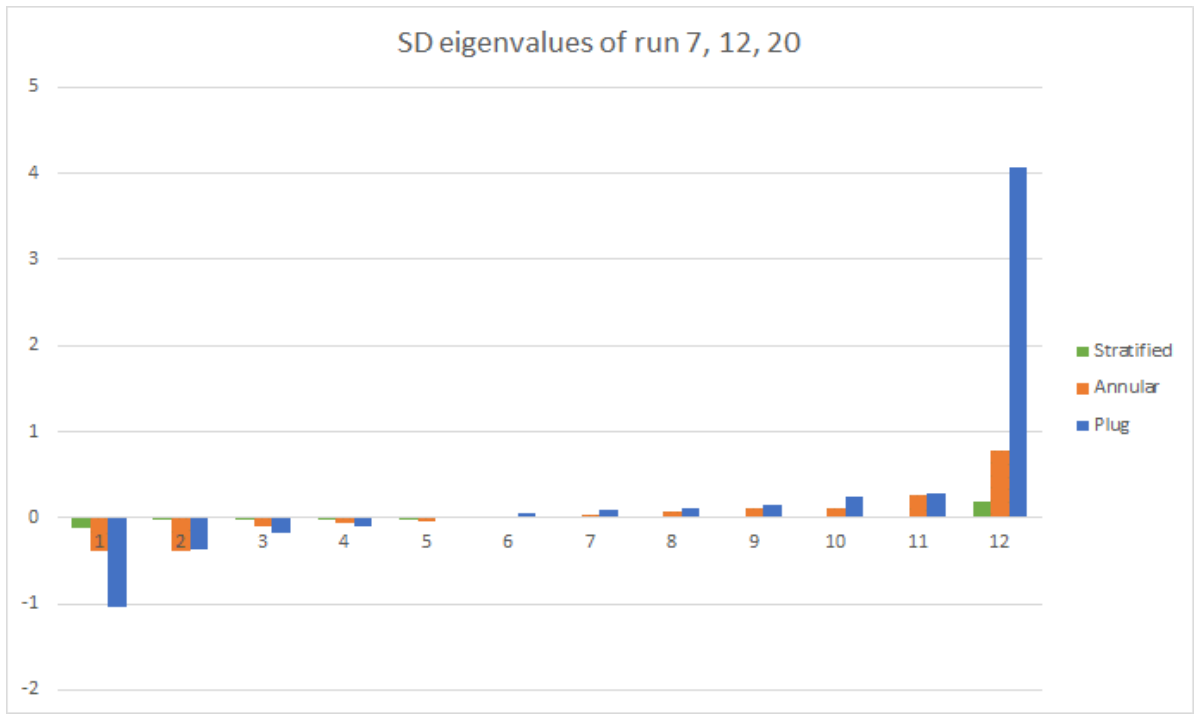


Figure 7-3: Eigenvalues of the standard deviation matrix of measurements 7, 12, 20. Data taken from ‘.anc’ plane 2

In Figure 7-3, three series of eigenvalues are displayed. One set is taken from a plug flow (measurement 20), the other from an annular flow (measurement 12) and the last one from a stratified flow (measurement 7).

It is clear that there is a significant difference between the values of the 12<sup>th</sup> eigenvalue. The value for the plug in this example is near five. The reason for the high value of the standard deviation is the great amplitude fluctuations in the signals.

$$\text{FlowPattern} = \text{Intermittent if } 12^{\text{th}} \text{ Eigenvalue of SD} > 1,15 \quad (7-1)$$

The algorithm will help determining whether the flow pattern is intermittent or not. The first criterion for the intermittent flow was set at 1.5. After comparing the result from the algorithm and the observations, we have decided to lower the value. The value 1.15 gives the best results. The criterion to separate plug from slug flows is not yet found.

### 7.1.2. Criteria for intermittent flows using gamma-ray data.

The gamma-ray sensor takes density measurements. These can be used to determine if a flow is intermittent.

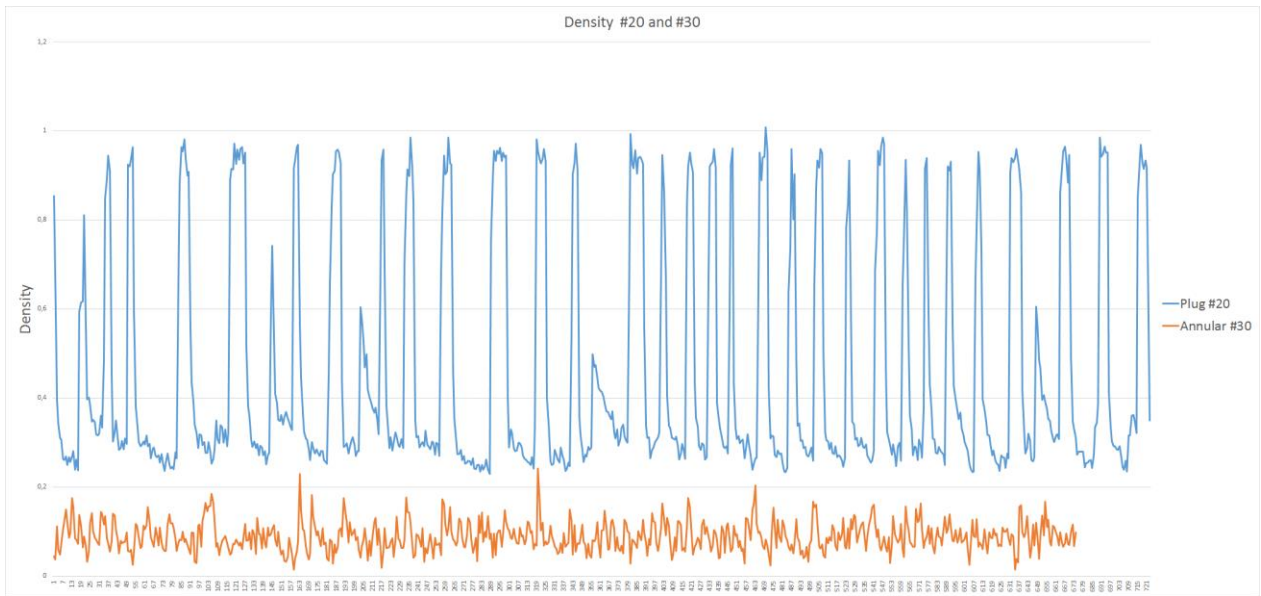


*Figure 7-4: Density chart of run 20 and 30. Blue line is plug flow run 20, orange is an annular flow run 30.*

In Figure 7-4, some density measurements are plotted. The blue line represent run 20 and is a plug flow, the orange line is run 30 and it shows the density measurements of an annular flow. In the graph, it is clear that the density measurements for the plug flow has many peaks. The peaks represent the plugs that flow through the pipes. If the plug passed the sensor, the level in the pipe will decrease, as shown by the density measurements. The annular flow has a lower density and does not have the peaks the plug flow has. Because an annular flow has a continuous distribution in the axial direction (see 3.2.3). For further analyzing, a FFT is applied on the time series data for density from the gamma ray measurements.

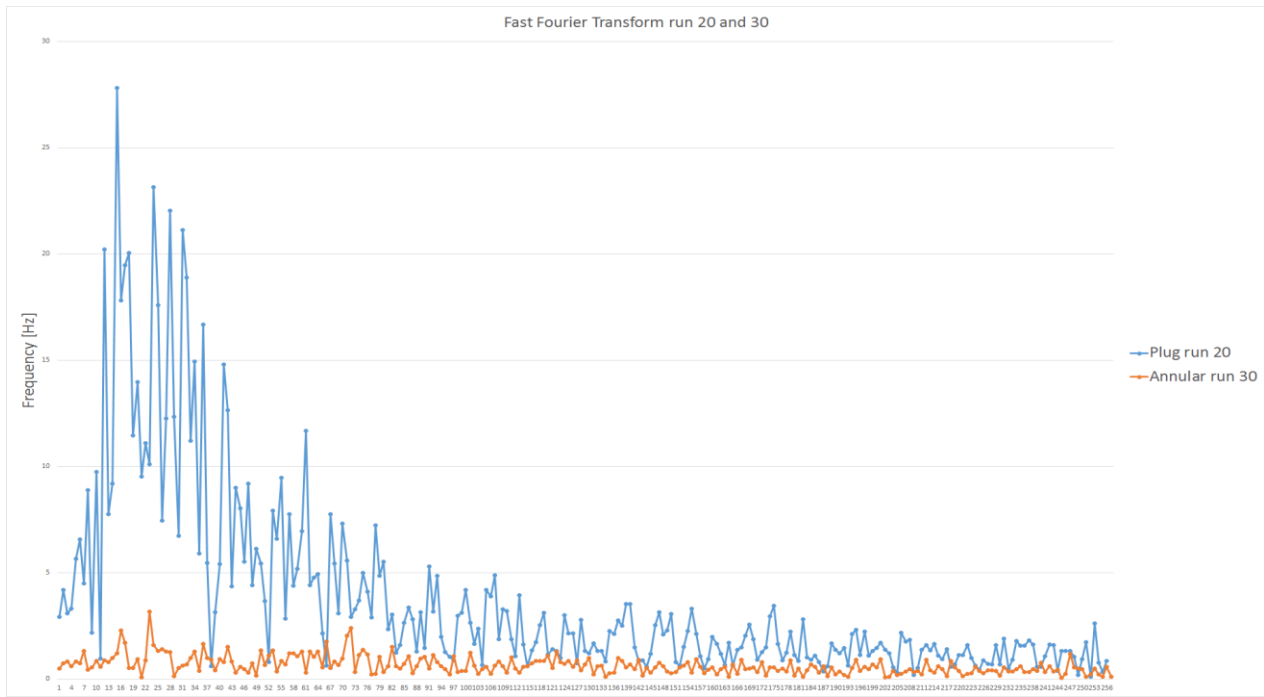


*Figure 7-5: FFT of the density chart in Figure 7-4. Blue is plug flow, orange is annular flow.*

Figure 7-5 shows the chart for the second to 256<sup>th</sup> frequencies coming out of the FFT. The dominance of low frequencies over the high frequencies seems to characterize intermittent flow (e.g. run 20 illustrated in Figure 7-5). As a result, in order to determine if the flow is an intermittent flow, the following parameter is used

$$Ratio_{FFT} = \frac{\sum_{2}^{111} y_{freq}}{\sum_{111}^{256} y_{freq}} \quad (7-2)$$

The ratio of the sums of the frequencies values is calculated. The sum is taken of the second until the one hundred and tenth-frequency value. This sum is then divided by the sum of the following 145 values. The following threshold is proposed:

$$Flow\ pattern = \text{intermittent\ flow\ if\ } Ratio_{FFT} > 2 \quad (7-3)$$

## 7.2. Annular and Wavy/Stratified flows

For the annular and wavy/stratified flow patterns, the data from the ECT sensor is used. The gamma-ray sensor data do not give enough information for the identification of the flow patterns. The difference between the flow patterns are very often of geometric nature, which can be obtained using tomographic systems.

The criterion for identification of annular flow regime is based on the ratio of the 11<sup>th</sup> eigenvalue with the 1<sup>st</sup> eigenvalue of the mean matrix. The eigenvalue vector is sorted from the smallest to the largest, as seen in Figure 7-3.

$$\varsigma = - \frac{(11^{\text{th}} \text{Eigenvalue of Mean Matrix})}{(1^{\text{th}} \text{Eigenvalue of Mean Matrix})} \quad (7-4)$$

Typically, the transition from stratified or wavy to annular flow is not a sharp boundary but more a transition area. Therefore, the parameter  $\varsigma$  will gradually increase. In order to set the threshold value, the video recordings of different runs were analyzed. If the top of the pipe were wetted, the flow pattern would be considered annular.

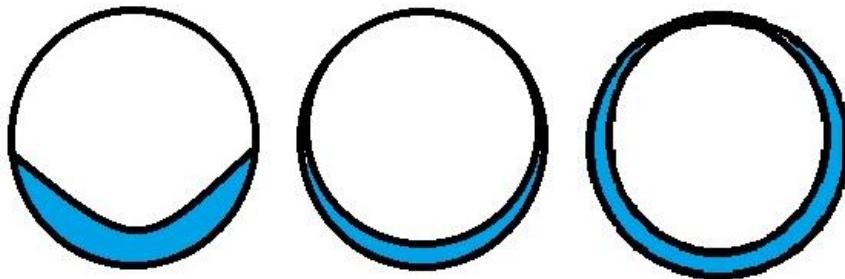


*Figure 7-6: Transition from stratified or wavy to annular. The water touches the top of the pipe in the right circle.*

In Figure 7-6, the transition is schematically shown. In the left circle, the water is starting to be pressed onto the wall of the pipe. The circle in the middle shows that the water is becoming a thin layer around the whole pipe but it does not yet touch the top of the pipe. The water touches the top of the pipe in the last circle. The last circle is considered annular, the other two are not. The parameter threshold for annular flow is found to be around  $\varsigma_{\text{thresh}} = 0.20$ .

Note that intermittent flows usually would be mistaken as annular flows using this criterion, but since the criterion for identification of intermittent flows is tested first, this confusion can be avoided.

In the algorithm, if the flow pattern is neither intermittent nor annular, it is classified as a wavy/stratified flow. A criterion for this flow patterns has not been found yet.

Table 7-1: The criteria found for the different flow patterns and their formulas

Flow regime	Criterion	Flow regime map
Intermittent (ECT sensor)	$12^{\text{th}} \text{ eigenvalue of } SD > 1,15$	
Intermittent (gamma-ray sensor)	$\text{Ratio}_{FFT} = \frac{\sum_2^{111} y_{freq}}{\sum_{111}^{256} y_{freq}}$ $\text{Ratio}_{FFT} > 2$	
Annular (ECT sensor)	$\zeta = -\frac{(11^{\text{th}} \text{ Eigenvalue of Mean Matrix})}{(1^{\text{th}} \text{ Eigenvalue of Mean Matrix})}$ $\zeta_{thresh} > 2$	

### 7.3. Success/fail test of the algorithm.

During the experiments, observations were made for the actual flow pattern. This was done by filming the transparent section of the pipe (see Figure 4-2) and by visual inspection. After the calculations are done and the algorithms have determined which flow pattern the flow was, a comparison is made between the observed flow pattern and the determined flow pattern. In this test, FFT test using gamma-ray signals is left out.

*Table 7-2: Success/fail test table, the measurements done with horizontal pipe and inclined pipe are separated.*

	Normalized Plane 1	Normalized Plane 2	Absolute Plane 1	Absolute Plane 2
Total	137	137	137	137
Wrong FP	35	15	49	26
Percentage Wrong	25,5%	10,9%	35,8%	19,0%
Straight Pipe	115	115	115	115
Wrong FP	27	7	36	18
Percentage Wrong	21,7%	6,1%	31,3%	15,7%
Angled Pipe	22	22	22	22
Wrong FP	8	8	13	8
Percentage Wrong	36,4%	36,4%	59,1%	36,4%

From Table 7-2, one can conclude that the best results are derived from the data out of the normalized plane 2 measurements. A possible reason for this is that, during the experiments bubbles were present in the front of the sensor. This was visible on the tomographic image of plane one in the ECT32v2 software. Therefore, data from plane 1 includes bubbles, which possibly influenced the measurements. In addition, it shows that the highest percentage of wrong flow patterns is found with inclined pipes.

In those experiments, the flow patterns did not behave as suspected, with high amplitude waves difficult to attribute to intermittent flows or wavy flows.

Additionally, the criteria have been derived from sets of experiments not including measurements with inclined pipes. This needs further investigation.

Furthermore, the wrong identification of the flow pattern for the horizontal pipes are usually flows that are near or in a transition area between two flow patterns. I.e. run 43 is determined to be an annular flow. In the visual observation, the flow pattern is determined to be a wavy flow. In run 44, the flow is determined to be an annular flow and was recognized as an annular flow. The difference between run 43 and 44 is that in run 44 the airflow rate was 0.2 kg/min higher than in run 43. Therefore, it is difficult to say if the observer made a wrong identification of the flow pattern or the algorithm did not work as desired. The transition between some of the flow patterns is very difficult to observe because it takes place in a transition area and is not a rapid shift between two flow patterns. It gradually changes (see Figure 3-1). Despite the intrinsic difficulty to draw a line between the different zones on the flow regime map that is obtained by the measurements (Figure 7-6), the similarity between the transition zones in the flow regime map generated, corresponds to the one found in the literature (Figure 5-1, for slightly smaller pipe diameter. 50mm). Because the diameters are not the same, it is expected that the transitions will shift for higher air and water velocities.

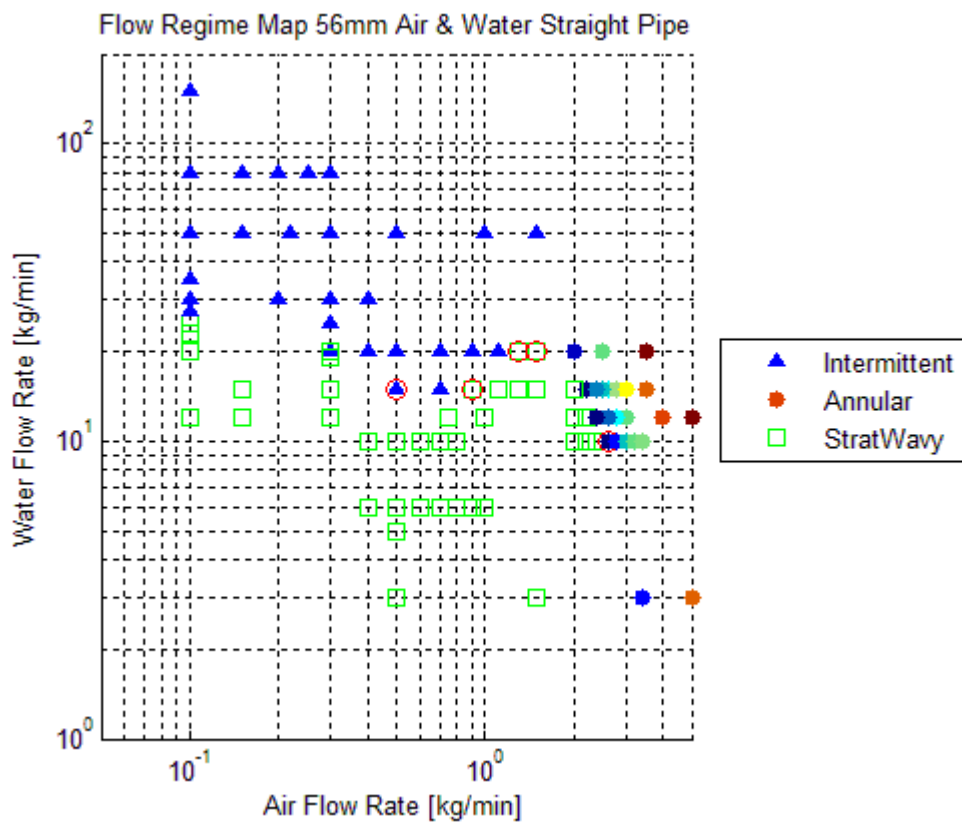


*Figure 7-7: Flow regime map with the flow pattern identification of a horizontal 56 mm pipe. The points on the plot with red circle around are the flow patterns that are false, according to the success fail test. The generation of this map is explained in Chapter 8. Based on analyzing 115 different measurements performed on the multiphase rig.*

## 8. Flow regime mapping

The results from the flow pattern algorithm (Chapter 7) will be used for making a flow regime map of the experiments performed. In the next paragraphs, the MATLAB code FlowRegimeMapping.m used for making the mapping is explained. Full code is found in Annex 5.

### 8.1. Data export from Excel to MATLAB

The data that will be used is imported from an Excel file. In the Excel file, a specific tab is made for the measurements taken with a horizontal pipe. This is important because the measurement from horizontal pipes cannot be mixed with measurements from inclined pipes.

```
%% Get data out the excel file
Measurements = xlsread('Flow_regime_identification.xlsx','horizontal_pipe');
```

Figure 8-1: MATLAB code for importing data out of Excel sheets

In the code that is presented in Figure 8-1 the name of the Excel file can be changed according to which file is needed. The values that are used come from the normalized eigenvalues in plane 2. (Chapter 6 for explanation)

Once the Excel-sheet is imported in MATLAB, the desired column will be selected. This is done using the following code.

```
%% Mapping with FP results
figure
Intermittent = Measurements(1:end,4);
Annular = Measurements(1:end,5);
StratWavy = Measurements(1:end,6);
SuccessorFail = Measurements(1:end,7);
Flow_rates=Measurements(1:end,1:2);
```

Figure 8-2: Importing the desired columns into a vector

The columns containing the 0 and 1 values, coming from the flow pattern algorithm are stored into columns with specific names. The flow rates and the success/fail test result are stored.

## 8.2. Mapping of flow regimes

After the different datasets are imported, they can be used for mapping the flow regimes.

The MATLAB code makes two plots. One from all the measurements taken without distinguishing which flow pattern it is and the other one with the distinction.

### 8.2.1. Mapping all measurements without flow pattern identification

With this scatterplot, all the measurements taken with the horizontal pipe are plotted using the following code:

```
%% Mapping All Measurements
Water = Measurements(1:end,1);
Air = Measurements(1:end,2);
figure
scatter(Air,Water);
grid on
set(gca,'xscale','log');
set(gca,'yscale','log');
title('Measurements taken with Multiphase flow rig Air & Water Straight Pipe');
xlabel('Air Flow Rate [kg/min]'); % x-axis label
ylabel('Water Flow Rate [kg/min]') % y-axis label
axis([0.05 5 1 200]);
```

Figure 8-3: MATLAB code for scatterplot all measurements

The scatterplots have logarithmic scale in the two axes. The two axes both have a determined length. This is done so all the mapping generated will have a similar look.

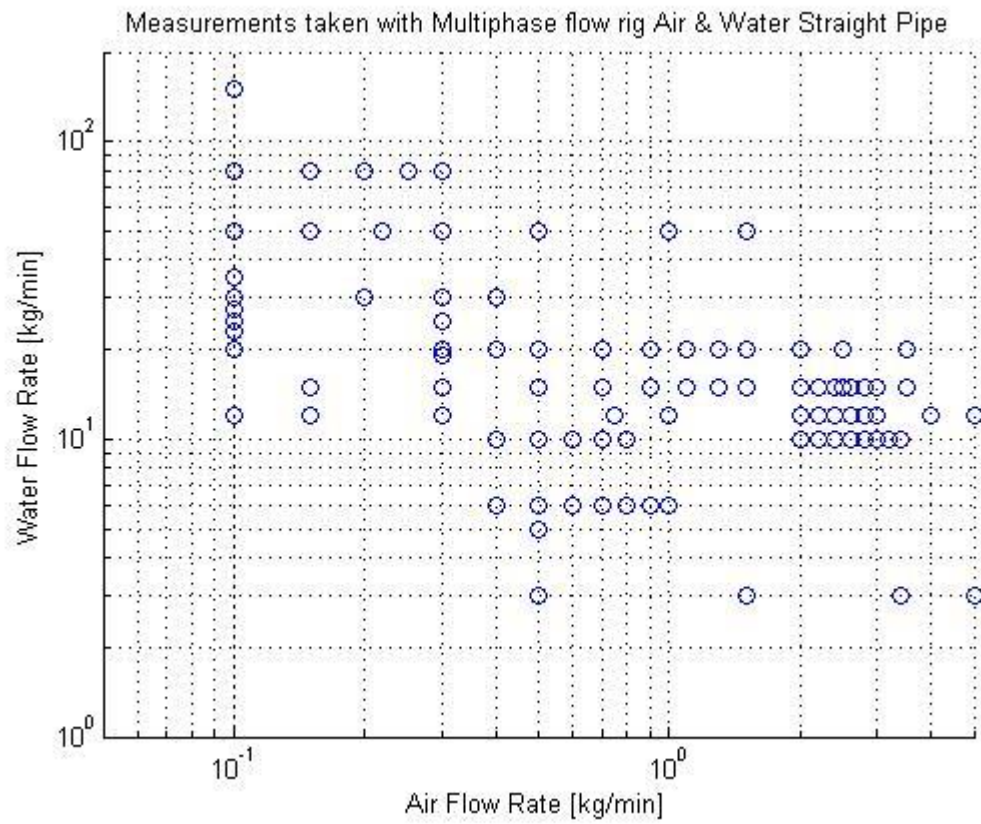


*Figure 8-4: Mapping of all measurements taken with horizontal pipe.*

In this plot, some measurements are not presented properly, because they have the same values of air and water velocity. The points overlap and there is no indication of the double point. This problem has not been solved yet.

This plot can be helpful to decide in which region more measurements needs to be taken. In addition, this plot can be made before the measurements are taken. This will perhaps help to design experiment sessions.

### 8.2.2. Mapping the flow regimes

The next mapping will be a flow regime map. This mapping will have the same points as the one shown in Figure 8-5. The difference will be a number of different colors and symbols to represent the flow pattern or a group of flow patterns. As of now, the algorithms splits the flow patterns into three different groups: intermittent flow (Plug and slugs), annular, stratified/wavy. The algorithm used in the Excel sheets determine which flow pattern it is. For giving the different points in the scatterplot the right coded color and symbols, these values are used. They are imported and stored into the vectors Intermittent, Annular and StratWavy (Figure 8-2).

The values of the flow rates and the success or fail test are stored as well. The assignment and plotting of the different points is done by following MATLAB code.

```
for i_index=1:length(Flow_rates)
    selectedRow = i_index;
    if Intermittent(selectedRow,1) == 1;
        scatter(Flow_rates(selectedRow,2),Flow_rates(selectedRow,1), '^', 'b', 'filled')
    elseif Annular(selectedRow,1) ~= 0;
        scatter(Flow_rates(selectedRow,2),Flow_rates(selectedRow,1), 40,Annular(selectedRow,1), 'filled', 'o')
    elseif StratWavy(selectedRow,1) == 1;
        scatter(Flow_rates(selectedRow,2),Flow_rates(selectedRow,1), 's', 'g')
    end
    hold on
    if SuccessorFail(selectedRow,1) == 1;
        scatter(Flow_rates(selectedRow,2),Flow_rates(selectedRow,1), 80, 'o', 'r')
    end
    hold on
end
```

*Figure 8-5: Assigning the flow patterns and plotting the different points in flow regime map*

In the MATLAB code, presented in Figure 8-5, the code will determine which flow pattern it is by searching for the columns that possesses a value equal to 1. Then the values of the velocities are plotted with a specific color and symbol code. The result is shown in Figure 8-6.

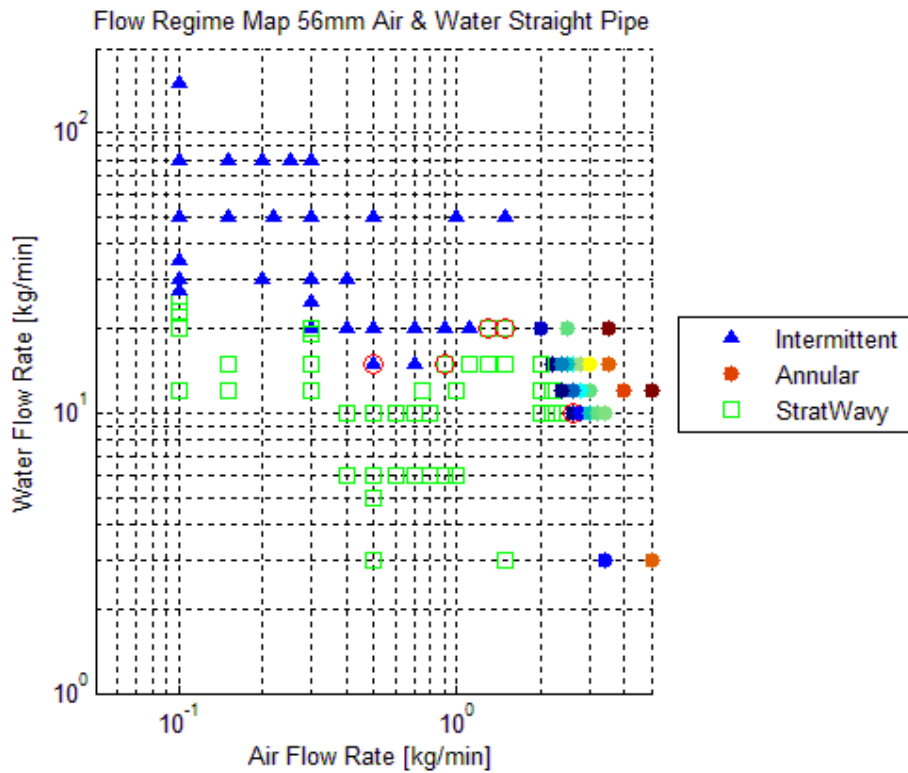


*Figure 8-6: Flow regime map with flow pattern identification of horizontal pipe 56 mm, based on 115 experiments runs in the multiphase rig.*

The legend in the plot explains which symbol is which flow pattern. If this flow regime map is compared with Figure 5-1, the imaginary lines between the different regions Intermittent, Annular and StratWavy have the same shape as the lines presented in this flow regime map given in [Mandhane et al., 1974], the straight line between StratWavy and SlugPlug for low air flow rate, the parabolic line between StratWavy and SlugPlug for medium air flow rate and the declining straight line between StratWavy and Annular.

The color of the annular points of the flow regime map gradually change. The meaning behind this is that the blue annular points are the least annular flows. The ‘annularity’ of the flow gradually increases if the air flow rate is increased. The points on the mapping will go from blue (low annularity) to red (high annularity), according to Figure 7-6.

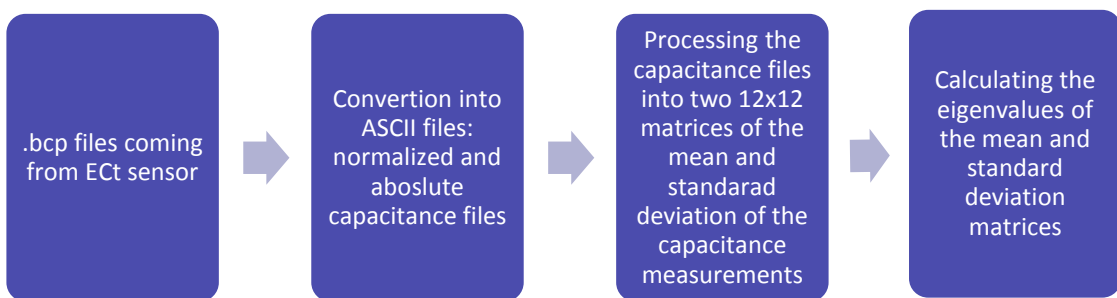
In Figure 8-6, five red circles are present. This is derived from the success/fail test of the flow pattern identification. This means that if a point in the map is red circled, the flow pattern that is observed varies from the flow pattern calculated with the algorithm. These points will need to be studied further. Also notice that in Table 6-2 there are seven wrong flow patterns found and in the mapping only five. This is because 4 runs that have wrong flow patterns are the same: run111/127 and run 112/run126.

# 9. Conclusion and future work

## 9.1. Conclusion

All the experiments performed use a horizontal pipe combined with water and air as the two different phases. The raw data, gathered from these experiments, needs to be processed in order to analyze it. There are a couple of different data sets gathered: the ECT sensor data, gamma-ray sensor data, flow rates and differential pressure sensor data.

The ECT sensor data will be processed using following steps:



Once all the eigenvalues are calculated, a parameter is searched that best characterizes the flow regime. For this, the gamma-ray sensor data and camera footage is used to see when a flow pattern goes over into another. This helps to set the threshold that best fits the algorithm.

Three criteria are found for flow patterns. Two criteria are found for intermittent flow patterns, one criterion is found for annular flows. Intermittent flow patterns include slug and plug flows. One criterion is found by using the eigenvalues of the standard deviation matrix, originating from the ECT sensor.

$$\text{FlowPattern} = \text{Intermittent if } 12^{\text{th}} \text{ Eigenvalue of SD} \geq 1,15$$

Another criterion is found by applying a FFT on the gamma-ray sensor data.

$$Ratio_{FFT} = \frac{\sum_2^{111} y_{freq}}{\sum_{111}^{256} y_{freq}}$$

The ratio of the sums of the frequency values is calculated. The sum is taken of the second until the one hundred and tenth-frequency value. This sum is than divided by the sum of the following 145 values. If the ratio is bigger than two, the flow pattern will be identified as an intermittent flow.

The third criterion that came out of the analysis is a criterion for annular flow. This uses eigenvalues of the mean matrix.

$$\varsigma = - \frac{(11^{\text{th}} \text{ Eigenvalue of Mean Matrix})}{(1^{\text{th}} \text{ Eigenvalue of Mean Matrix})}$$

If  $\varsigma$  is bigger equal to or bigger than 0.2, the flow will be an annular flow. Note that intermittent flows usually would be confused with annular flows with this criterion. However, since the criterion for identification of intermittent flows is tested first, they can be discarded.

With these criteria, the fast recognition of flow patterns is possible. A criterion for wavy and stratified flows has not been found yet. Nevertheless, as in the experiments, if only three type of low patterns (intermittent, annular, strat/wavy) are examined, only two criteria are needed.

The algorithm for flow recognition can be used to obtain flow regime maps, specific for a given flow rig. In this project, a large number of measurements have been analyzed with varying input mass flow rates and obtained the following flow regime map.

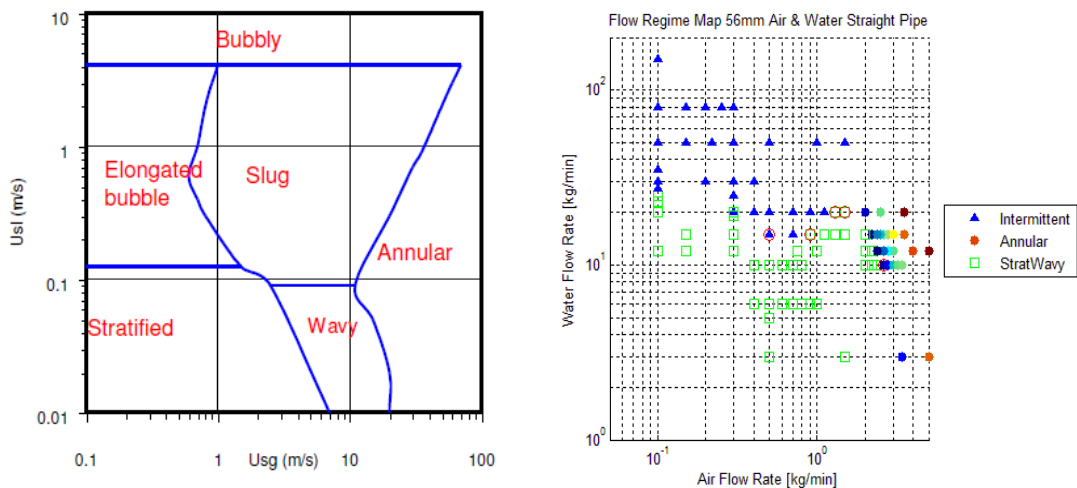


*Figure 9-1: Mandhane map [Mandhane et al., 1974] on the left and the flow regime map generated for flow rig at USN, Porsgrunn on the right*

There is a slight but noticeable difference with the Mandhane map (Figure 9-1 on the left), so the reader will realize the potential of such flow regime identification techniques for generating flow regime maps specific for a given installation.

The transition criterion between the different flow patterns are not found in this thesis. It is hard to determine when a specific flow pattern starts to transition into another one.

In this thesis, some experiments are taken with an inclined pipe. The algorithm was tested on the data sets but the result were not promising. The success/fail rate of the flow pattern was high.

## **9.2. Future work**

- Finding the transition criteria for the different flow patterns.
- Validating the criteria with different sensors and pipe diameters.
- Studying the behavior of flow patterns in angled pipes and trying to fine-tune the criteria to give better results.
- Combining the analyzing method and flow pattern criteria to get a direct recognition of the flow pattern out of the sensors. Also, combine the criteria, coming from the ECT data and gamma-ray data, for intermittent flows.
- Perform similar test with other modalities, i.e. ERT, EIT etc.

# References/bibliography

Brennen, C.E. (2005). *Fundamentals of Multiphase Flows*. Pasadena, California: Cambridge University Press. ISBN 0521-848040

Fang, W., Cumberbatch, E., (2005) Matrix properties of data from electrical capacitance tomography. *Journal of Engineering Mathematics* (51)

Hansen, M., Kumara, A.S., Pradeep, C., (2011) *Operating Procedure, PH-RN Multiphase flow rig I.*

Ismail, I. (2005). Tomography for multi-phase flow measurement in the oil industry. *Flow Measurement and Instrumentation* (16)

Johansen, G.A. (2015). *Industrial Tomography: Systems and Applications*. 197-222, ISBN 978-1-78242-8

Mandhane, J.M. (1974). A flow pattern map for gas-liquid flow in horizontal pipes. *International Journal of Multiphase Flow*

Marashdeh, Q. (2007). A multimodal tomography system based on ECT sensors. *IEEE Sensors Journal* (vol. 7)

NFOGM, The Norwegian Society for Oil and Gas Measurements. (2005). *Handbook of Multiphase Flow Metering*, ISBN 82-91341-89-3

Pradeep, C. (2015). *Tomographic approach to automatic and non-invasive flow regime identification*. TUC PhD thesis.

Schlieper, G. (2000). Principles of gamma ray densitometry. *MPR*

# List of tables and figures

## Figures

Figure 2-1: Twin plane tomographic measurement system of a multiphase flow [Ismail et al., 2005].

Figure 2-2: Twin plane ECT sensor mounted in the multiphase flow rig located in the process hall at USN, Porsgrunn.

Figure 2-3: Schematic representation of an 8-electrode ECT-sensor [Ismail et al., 2005]

Figure 2-4: Gamma-ray sensor mounted in the multiphase flow rig in the process hall.

Figure 3-1: Example of a flow regime map for a horizontal pipe. Hatched regions: observed boundaries zones, continuous lines: theoretically predicted boundaries.

[Brennen C. E., 2005]

Figure 3-2: Flow regimes for air/water mixture in a horizontal pipe. G is for gaseous phase, L for liquid phase [Brennen C. E., 2005]

Figure 4-1: Piping and Instrumentation Diagram (PID) of the multiphase flow facility at USN [Pradeep et al., 2014]

Figure 4-2: Test section with sensor placements as part of the titled pipe with multiphase flow. Transparent section for high-speed camera base studies and visual observations, multimodal tomographic systems at the far right of the pipe. [Pradeep et al., 2014].

Figure 4-3: Measurement principle of ECT sensor. Electrode 1 is excited with  $V_s$  and other electrodes are earthed. [Pradeep et al., 2014]

Figure 5-1: Flow regime map for a horizontal 50 mm pipe, air and water 20°C, based on [Mandhane et al., 1974]

Figure 6-1: Screen capture from ASCII output ‘.aac’ file generation

Figure 6-2: Screen capture of ASCII output ‘.anc’ file generation

Figure 6-3: Multiple files directory load and building of the eigenvalue matrices for all the eigenvalue vectors of the different runs

Figure 6-4: Generation of 12x12x6000 matrix including the calculation of the diagonal term and the calibration

Figure 6-5: Calculating the mean matrix, standard deviation matrix and their eigenvalues. These values will be written into the zero matrices created in the first part of the code (6.4.1)

Figure 7-1: Eigenvalue graph of standard deviation matrices. Green represents stratified and wavy flows, orange represents annular flow and blue represents slug and plug flows.

Figure 7-2: Eigenvalue graph of mean matrices. Green represents stratified and wavy flows, orange represents annular flow and blue represents slug and plug flows.

Figure 7-3: Eigenvalues of the standard deviation matrix of measurements 7, 12, 20. Data taken from ‘.anc’ plane 2

Figure 7-4: Density chart of run 20 and 30. Blue line is plug flow run 20, orange is an annular flow run 30.

Figure 7-5: FFT of the density chart in Figure 7-4. Blue is plug flow, orange is annular flow.

Figure 7-6: Transition from stratified or wavy to annular. The water touches the top of the pipe in the right circle.

Figure 7-7: Flow regime map with the flow pattern identification of a horizontal 56 mm pipe. The points on the plot with red circle around are the flow patterns that are false, according to the success fail test. The generation of this map is explained in Chapter 8. Based on analyzing 115 different measurements performed on the multiphase rig.

Figure 8-1: MATLAB code for importing data out of Excel sheets

Figure 8-2: Importing the desired columns into a vector

Figure 8-3: MATLAB code for scatterplot all measurements

Figure 8-4: Mapping of all measurements taken with horizontal pipe

Figure 8-5: Assigning the flow patterns and plotting the different points in flow regime map

Figure 8-6: Flow regime map with flow pattern identification of horizontal pipe 56 mm, based on 115 experiments runs in the multiphase rig.

Figure 9-1: Mandhane map [Mandhane et al., 1974] on the left and the flow regime map generated for flow rig at USN, Porsgrunn

## Tables

Table 3-1: Description of the different flow patterns found in horizontal pipes from our experimental studies and [Brennen C. E., 2005].

Table 4-1: Pump specifications for different pumps in the flow loop. The specific pump can be found in the diagram using the pump number. [Hansen et al., 2011]

Table 4-2: Pipe dimensions in the vicinity of the tomographic systems [Hansen et al., 2011]

Table 6-1: Normalized capacitance data from the second plane of the ECT sensor run 001.

Table 6-2: Normalized capacitance data from run001. The initial data is mirrored around the diagonal term.

Table 6-3: Two sets of the 6000 capacitance data processed by the MATLAB code. This is a part of the 66000x11 matrix, called matrix1 in the MATLAB code.

Table 7-1: The criteria found for the different flow patterns and their formulas

Table 7-2: Success/fail test table, the measurements done with horizontal pipe and inclined pipe are separated.

# Annexes

Annex 1: <Master thesis description.>

Campus Porsgrunn/Faculty of Technology  
Department of Electrical Engineering, IT and Cybernetics

## FMH 606 Master's Thesis

**Title:** Process Tomometric Data Fusion with Multimodal Sensor Suite in Multiphase flow studies

**USN supervisor:** Saba Mylvaganam, Kjell Joar Alme (only on need basis),

**External partner:** Professor Geir Elseth, STATOIL / PhD Research Fellow Antoine DUPRE, CEA Cadarache, Institut Fresnel (France)

### **Task description:**

Focus in this project is the multimodal tomometry (ECTm and ERTm) in studying various features of multi-phase flow, but bypassing image processing and incorporating time series data from high-speed camera, gamma meter and some conventional sensors. This means that the focus will be on exploiting patterns in the actual time series of raw data from the array of multimodal sensors or their other mathematical properties. Considerable work has been done earlier at USN. The present thesis should strive to add value to existing results and findings achieved particularly by students and staff at USN. Real times processing of time series, data mining approach, wavelets, and matrix methods are some keywords associated with this project. The goals for the present thesis project are the following:

- (1) Survey of multimodal process tomometry with focus on its application to multi-phase flow
- (2) Understanding and describing the basic features of the process multimodal systems in the Sensor Lab at TUC including the programs developed by TUCs collaborators and PhD students.
- (3) Generating data sets using multi-phase flow rigs at TUC and analysing them for flow regime, bubble and slug studies
- (4) Online data acquisition and processing with multi-modal sensor suite
- (5) A brief survey of flow regimes in multiphase flow in tabular form with own sketches and at least some own photos/videos using TUC flow rigs.
- (6) Analysis of data with focus on slug and bubble characterization and means of studying wavy flow
- (7) Characterization of plug vs slug flow
- (8) Criteria for identification of transition from stratified to wavy flow. Validation with high speed camera
- (9) Mapping of the flow regimes for the USN flow rig, with gradual transitions based on criteria found in (8)
- (10) Submitting a report using the guidelines and template of USN with systematically archived data sets and software

### **Task background:**

Multimodal sensor suites for multiphase flow is found increasingly in the oil and gas & process industries. TUC has the latest equipment on multimodal and capacitance based tomography. Recently, a modern Gamma ray based measurement system has been added to the sensor suite on the multiphase flow rig. There will be close collaboration with manufacturers of process tomographic equipment in the UK. Currently, USN is conducting a measurement campaign in collaboration with University of Stavanger.

### **Student category:**

This work is suitable for both SCE/PEM students with some interest in mathematical techniques. *As the work entails continuous lab work and program development, students need to be at USN throughout the term. It is mandatory that students have weekly meeting with at least one the supervisors in the lab.*

### **Practical arrangements:**

Necessary hardware and software will be provided by USN. Work will be performed in Sensor Lab and Process Hall where the multiphase flow facilities are available.

However, possible interaction with process tomography research groups in Norway and abroad is also envisaged. Students need to familiarise themselves with the earlier work done at USN and USNs collaborators in the field. Some data sets from real industrial measurements may be available in the final stages of the thesis work.

### **Signatures:**

Student (date and signature): Stijn Vyncke  
12.02.2016

Supervisor (date and signature):  
12.02.2016

Annex 2: <All measurements taken during sessions, colour code green means data represented for that column is taken, red means it is not taken>

Sample	Water Flow Rate	Air Flow rate	Flow regime		ECT	Process parameters	Gamma	High-Speed Camera
#1	80	0	Full	1_01	05.02.2016			
#2	80	0,15	Plug	1_02				
#3	12	4	Annular	1_03				
#4	12	2	Wavy	1_04				
#5	12	1	Wavy	1_05				
#6	12	0,1	Stratified	1_06				
#7	12	0,15	Stratified	2_01	10.02.2016			
#8	12	0,3	Stratified	2_02				
#9	12	0,75	Wavy	2_03				
#10	12	1	Wavy	2_04				
#11	12	2	Wavy	2_05				
#12	12	3	Annular	2_06				
#13	12	4	Annular	2_07				
#14	12	5	Annular	2_08				
#15	15	0,15	Stratified	2_09				
#16	35	0,1	Plug	2_10				
#17	50	0,1	Plug	2_11				
#18	150	0,1	Plug	2_12				
#19	80	0,1	Plug	3_01	17.02.2016			
#20	80	0,15	Plug	3_02				
#21	80	0,2	Slug	3_03				
#22	80	0,25	Slug	3_04				
#23	80	0,3	Slug	3_05				
#24	30	0,1	Plug	3_07				
#25	30	0,2	Plug	3_08				
#26	30	0,3	Slug	3_09				
#27	30	0,4	Slug	3_10				
#28	15	2	Wavy	3_11				
#29	15	2,2	Annular	3_12				
#30	15	2,4	Annular	3_13				
#31	15	2,6	Annular	3_14				
#32	15	2,8	Annular	3_15				
#33	15	3	Annular	3_16				
#34	12	3	Annular	3_17				
#35	12	2,8	Annular	3_18				
#36	12	2,6	Annular	3_19				
#37	12	2,4	Annular	3_20				

Sample	Water Flow Rate	Air Flow rate	Flow regime		ECT	Process parameters	Gamma	High-Speed Camera
#38	12	2,2	Wavy	3_21				
#39	12	2	Wavy	3_22				
#40	10	2	Wavy	4_01	18.02.2016			
#41	10	2,2	Wavy	4_02				
#42	10	2,4	Wavy	4_03				
#43	10	2,6	Wavy	4_04				
#44	10	2,8	Annular	4_05				
#45	10	3	Annular	4_06				
#46	10	3,2	Annular	4_07				
#47	10	3,4	Annular	4_08				
#48	3	3,4	Annular	4_09				
#49	3	5	Annular	4_10				
#50	3	1,5	Wavy	4_11				
#51	3	0,5	Stratified	4_12				
#52	5	0,5	Stratified	4_13				
#53	10	0,4	Stratified	5_01	26.02.2016			
#54	10	0,5	Stratified	5_02				
#55	10	0,6	Wavy	5_03				
#56	10	0,7	Wavy	5_04				
#57	10	0,8	Wavy	5_05				
#58	6	0,4	Stratified	5_06				
#59	6	0,5	Stratified	5_07				
#60	6	0,6	Stratified	5_08				
#61	6	0,7	Wavy	5_09				
#62	6	0,8	Wavy	5_10				
#63	6	0,9	Wavy	5_11				
#64	6	1	Wavy	5_12				
#65	30	0,3	Plug	5_13				
#66	25	0,3	Plug	5_14				
#67	20	0,3	Plug	5_15				
#68	19	0,3	Wavy	5_16				
#69	20	0,1	Stratified	5_17				
#70	23	0,1	Stratified	5_18				
#71	25	0,1	Stratified	5_19				
#72	27,5	0,1	Plug	5_20				
#73	27,5	0,1	Slug	6_1	04.03.2016			
#74	25	0,1	Slug	6_2				
#75	23	0,1	Slug	6_3				
#76	15	0,1	Slug	6_4				
#77	12	0,1	Slug	6_5				
#78	12	0,3	Slug	6_6				

Sample	Water Flow Rate	Air Flow rate	Flow regime		ECT	Process parameters	Gamma	High-Speed Camera
#79	12	1,5	Slug	6_7				
#80	12	1,7	Annular	6_8				
#81	12	1,9	Annular	6_9				
#82	12	2,2	Annular	6_10				
#83	12	2,5	Annular	6_11				
#84	12	3	Annular	6_12				
#85	30	0,1	Wavy	6_13				
#86	30	1	Wavy	6_14				
#87	30	1,5	Wavy	6_15				
#88	30	2	Slug	6_16				
#89	30	2,5	Slug	6_17				
#90	30	3	Slug	6_18				
#91	50	0,1	Plug	7_1	14.03.2016			
#92	50	0,15	Plug	7_2				
#93	50	0,22	Slug	7_3				
#94	50	0,3	Slug	7_4				
#95	50	0,5	Slug	7_5				
#96	50	1	Slug	7_6				
#97	50	1,5	Slug	7_7				
#98	15	0,3	Wavy	7_8				
#99	15	0,5	Wavy	7_9				
#100	15	0,7	Slug	7_10				
#101	15	0,9	Slug	7_11				
#102	15	1,1	Wavy	7_12				
#103	15	1,3	Wavy	7_13				
#104	15	1,5	Wavy	7_14				
#105	15	2	Wavy	7_15				
#106	15	2,5	Annular	7_16				
#107	15	3,5	Annular	7_17				
#108	20	3,5	Annular	7_18				
#109	20	2,5	Annular	7_19				
#110	20	2	Annular	7_20				
#111	20	1,5	Annular	7_21				
#112	20	1,3	Annular	7_22				
#113	20	1,1	Slug	7_23				
#114	20	0,9	Slug	7_24				
#115	20	0,7	Slug	7_25				
#116	20	0,5	Slug	7_26				
#117	20	0,3	Slug	7_27				
#118	80	0,2	Slug	8_1	05.04.2016			
#119	19	0,3	Wavy	8_2				
#120	20	0,3	Wavy	8_3				

Sample	Water Flow Rate	Air Flow rate	Flow regime		ECT	Process parameters	Gamma	High-Speed Camera
#121	20	0,3	Wavy	8_4				
#122	20	0,4	Slug	8_5				
#123	20	0,7	Slug	8_6				
#124	20	0,9	Slug	8_7				
#125	20	1,1	Slug	8_8				
#126	20	1,3	Annular	8_9				
#127	20	1,5	Annular	8_10				
#128	20	2	Annular	8_11				
#129	15	3	Annular	8_12				
#130	15	2,4	Annular	8_13				
#131	15	0,7	Slug	8_14				
#132	15	0,3	Wavy	8_15				
#133	12	2,4	Annular	8_16				
#134	12	1,5	Slug	8_17				
#135	30	2	Slug	8_18				
#136	30	2,5	Slug	8_19				
#137	30	3	Slug	8_20				

Annex 3: <MATLAB code for analysing the data coming from the ECT sensors ASCII files.

This generates the different matrices and calculates the eigenvalues of those matrices.

This MATLAB code is saved as ECTMeasurementAnalysis.m>

```
clear all;clc

%% READ DATA, BUILD MATRIX
%%% absolute measurements (aac files)
%%%%% %%%%%% %%%%%% %%%%%% %%%%%% %%%%%% %%%%%% %%%%%% %%%%%% %%%%%%
% filename='run01.aac';
% calibration_water=[-5740.61120500007 1104.93015833342
578.206006666639 481.23218666647 406.35548333323 353.644813333306
352.605391666659 357.763081666664 384.64062833341 451.410149999991
588.803305000067 681.020000000017;1104.93015833342 -7559.07732333367
1299.48617166666 810.362080000008 625.370739999967 513.058311666700
484.744071666695 467.783123333348 477.668788333364 527.632586666688
627.754101666745 620.287190000072;578.206006666639 1299.48617166666 -
7347.90160500000 1335.20949833334 763.173566666673 563.090226666692
498.133773333329 452.341148333332 436.337711666664 455.154606666652
505.979474999986 460.789420000030;481.23218666647 810.362080000008
1335.20949833334 -7826.97055499986 1412.62997833339 772.895656666576
618.214194999976 525.936063333293 478.352739999989 471.182953333323
495.105005000026 425.850198333295;406.355483333323 625.370739999967
763.173566666673 1412.62997833339 -7659.36638000003 1190.79000000003
787.418996666641 610.129170000021 515.832126666686 480.245294999975
475.745119999972 391.675903333342;353.644813333306 513.058311666700
563.090226666692 772.895656666576 1190.79000000003 -7235.76800499989
1199.96999999994 744.835111666662 574.089573333295 494.925571666685
465.359303333329 363.109436666672;352.605391666659 484.744071666695
498.133773333329 618.214194999976 787.418996666641 1199.96999999994 -
7497.51443999983 1320.91779999994 750.645384999980 588.422390000049
515.007984999955 381.434451666668;357.763081666664 467.783123333348
452.341148333332 525.936063333293 610.129170000021 744.835111666662
1320.91779999994 -7541.27703833319 1305.25303666669 749.779951666596
594.665198333314 411.873353333330;384.640628333341 477.668788333364
436.337711666664 478.352739999989 515.832126666686 574.089573333295
750.645384999980 1305.25303666669 -7436.95151166671 1288.63949500004
750.673913333304 474.818113333368;451.41014999991 527.632586666688
455.154606666652 471.182953333323 480.245294999975 494.925571666685
588.422390000049 749.779951666596 1288.63949500004 -7432.52085500004
1312.84366500000 612.284190000041;588.803305000067 627.754101666745
505.979474999986 495.105005000026 475.745119999972 465.359303333329
515.007984999955 594.665198333314 750.673913333304 1312.84366500000 -
7442.3315333333 1110.39448166663;681.020000000017 620.287190000072
460.789420000030 425.850198333295 391.675903333342 363.109436666672
381.434451666668 411.873353333330 474.818113333368 612.284190000041
1110.39448166663 -5933.53673833347];
% calibration_air=[-1266.09402666661 575.521314999964 27.7267666666646
31.6006933333351 14.5850299999988 6.39741833333366 10.7852833333325
11.1080816666677 11.8748249999994 13.8192800000007 66.2163916666654
496.458941666645;575.521314999964 -1396.21729999995 630.367421666656
56.3067266666697 30.6402800000014 3.84743000000025 0.108226666666669
16.0893499999989 4.8821266666638 -3.8010283333343 27.2640399999993
54.9914116666630;27.7267666666646 630.367421666656 -1390.44603333336
613.208341666704 33.2459533333351 20.1670249999984 -1.69430000000002
4.93107833333347 12.5205366666667 1.19008999999994 25.3355783333337
23.4475416666660;31.600693333351 56.3067266666697 613.208341666704 -
1447.88082500009 615.228403333387 45.5864116666623 39.5137283333377 -
3.83307000000008 32.6297699999972 11.6608616666670 0.681909999999952
5.29704833333372;14.5850299999988 30.6402800000014 33.2459533333351
```

```

615.228403333387 -1414.12270500001 609.148511666623 50.1784016666669
1.64375666666657 30.9904750000002 7.15161333333287 21.5660233333340 -
0.255743333333322;6.39741833333366 3.84743000000025 20.1670249999984
45.5864116666623 609.148511666623 -1371.11389499992 605.372493333298
40.5484133333362 17.9543916666686 16.0216733333319 -0.179221666666656
6.24934833333332;10.785283333325 0.10822666666669 -1.69430000000002
39.5137283333377 50.1784016666669 605.372493333298 -1421.67688499997
633.80734333334 48.5661533333360 33.9140933333340 -0.1848999999999999
1.31036166666662;11.1080816666677 16.0893499999989 4.9310783333347 -
3.83307000000008 1.6437566666657 40.5484133333362 633.807343333334 -
1396.54035833333 636.322559999987 31.2720666666692 14.9900316666674
9.66074666666586;11.8748249999994 4.88212666666638 12.5205366666667
32.6297699999972 30.9904750000002 17.9543916666686 48.5661533333360
636.322559999987 -1458.54037499994 620.901019999954 39.2311016666645
2.66741500000008;13.8192800000007 -3.80102833333343 1.19008999999994
11.6608616666670 7.15161333333287 16.0216733333319 33.9140933333340
31.2720666666692 620.901019999954 -1421.25349833332 633.289686666697
55.8341416666675;66.2163916666654 27.2640399999993 25.3355783333337
0.681909999999952 21.5660233333340 -0.17922166666656 -
0.184899999999999 14.9900316666674 39.2311016666645 633.289686666697 -
1429.73831666670 601.527675000004;496.458941666645 54.9914116666630
23.4475416666660 5.2970483333372 -0.25574333333322 6.2493483333332
1.31036166666662 9.66074666666586 2.66741500000008 55.8341416666675
601.527675000004 -1257.1888833331];
%%% normalized absolute measurements (anc files)
%%%%%%% normalized absolute measurements (anc files)
% filename='run01.anc';
calibration_water=[-12.1191911666668 1.09318599999992 1.09433183333337
1.0272778333336 1.09491200000002 1.23082716666660 1.05654733333319
1.02777033333335 1.03956116666664 1.05448216666672 1.05729533333324
1.34299999999989;1.09318599999992 -11.6956126666672 1.12630833333346
1.01750000000002 1.07901599999995 1.21202416666684 1.03699233333336
1.00503933333342 1.0140706666673 1.0252681666659 1.02490533333328
1.06130233333326;1.0943318333337 1.1263083333346 -12.1308506666665
1.11052466666666 1.14189716666658 1.26785966666668 1.08305999999991
1.04500883333339 1.05100950000009 1.0606628333333 1.05709566666654
1.09309216666658;1.0272778333336 1.01750000000002 1.11052466666666 -
11.6346560000000 1.14535749999998 1.23257350000011 1.03808299999995
1.00072500000010 1.00528633333339 1.01131683333329 1.0078843333330
1.03812699999996;1.09491200000002 1.0790159999995 1.14189716666658
1.14535749999998 -12.376422666660 1.35599999999994 1.1345176666674
1.08448533333329 1.0770968333348 1.0821233333341 1.07293650000007
1.10808033333343;1.23082716666660 1.21202416666684 1.26785966666668
1.23257350000011 1.35599999999994 -13.8005053333339 1.34799999999996
1.24583816666672 1.22929000000000 1.2204814999995 1.21426916666666
1.24334200000007;1.0565473333319 1.03699233333336 1.08305999999991
1.03808299999995 1.1345176666674 1.34799999999996 -12.092188333329
1.1248133333331 1.0732546666670 1.0646844999994 1.0549963333338
1.07723916666681;1.0277703333335 1.00503933333342 1.04500883333339
1.00072500000010 1.08448533333329 1.24583816666672 1.1248133333331 -
11.7495996666667 1.0865333333342 1.0488903333330 1.0310286666663
1.04946700000004;1.03956116666664 1.01407066666673 1.05100950000009
1.00528633333339 1.0770968333348 1.22929000000000 1.07325466666670
1.08653333333342 -11.800160833337 1.1066473333332 1.05042150000011
1.06698950000000;1.05448216666672 1.02526816666659 1.0606628333333
1.01131683333329 1.0821233333341 1.2204814999995 1.0646844999994
1.04889033333330 1.1066473333332 -11.8676095000001 1.11100133333327
1.08205116666674;1.0572953333324 1.02490533333328 1.0570956666654
1.0078843333330 1.07293650000007 1.2142691666666 1.0549963333338
1.0310286666663 1.05042150000011 1.1110013333327 -11.8209775000004
1.13914333333341;1.34299999999989 1.0613023333326 1.09309216666658
1.03812699999996 1.1080803333343 1.24334200000007 1.07723916666681

```

```

1.04946700000004 1.06698950000000 1.08205116666674 1.13914333333341 -
12.3018340000004];
calibration_air=[-0.161968000000000 0.042121000000019 -
0.0309658333333366 0.029475999999995 0.0109780000000009 -
2.50000000000000e-06 0.0148890000000004 0.0119320000000004
0.0049931666666640 -0.0141861666666666 0.0260275000000009
0.066705833333347;0.042121000000019 -0.11409933333337
0.0561765000000006 0.014680666666670 0.0220570000000017 -
0.0138876666666667 -0.0150225000000005 0.0200264999999989 -
0.00604050000000019 -0.0320140000000018 0.0090498333333361
0.0169524999999995;-0.0309658333333366 0.0561765000000006 -
0.0643469999999987 0.0511351666666615 -0.0160815000000008
0.0080018333333379 -0.026431499999998 -0.00689550000000001
0.0130823333333339 -0.019289333333343 0.026003333333343
0.0096114999999994;0.029475999999995 0.014680666666670
0.0511351666666615 -0.183153666666665 0.0549093333333381
0.00382700000000015 0.0365135000000026 -0.0296778333333337
0.052157333333347 0.0074371666666676 -0.0187505000000015 -
0.0185541666666682;0.010978000000009 0.0220570000000017 -
0.0160815000000008 0.0549093333333381 -0.124811500000002
0.0398688333333307 0.0064006666666683 -0.032412833333324
0.0420155000000015 -0.00384250000000016 0.0319840000000019 -
0.0310650000000034;-2.50000000000000e-06 -0.013887666666667
0.0080018333333379 0.00382700000000015 0.039868833333307 -
0.039931999999975 0.029181499999989 -0.0079860000000044 -
0.00073766666666635 0.013177666666671 -0.018999833333350 -
0.0125111666666671;0.014889000000004 -0.0150225000000005 -
0.026431499999998 0.0365135000000026 0.0064006666666683
0.029181499999989 -0.090823833333324 0.0559170000000003
0.00605350000000019 0.029576333333331 -0.020258499999994 -
0.0259951666666674;0.011932000000004 0.020026499999989 -
0.00689550000000001 -0.029677833333337 -0.032412833333324 -
0.0079860000000044 0.055917000000003 -0.033348499999991
0.051081666666609 -0.018257666666675 -0.0038086666666683 -
0.0065701666666680;0.0049931666666640 -0.0060405000000019
0.013082333333339 0.052157333333347 0.0420155000000015 -
0.00073766666666635 0.00605350000000019 0.051081666666609 -
0.157067166666666 0.038772999999959 -0.00666483333333344 -
0.037646333333372;-0.014186166666666 -0.0320140000000018 -
0.019289333333343 0.0074371666666676 -0.0038425000000016
0.013177666666671 0.029576333333331 -0.018257666666675
0.038772999999959 -0.066367833333313 0.0406636666666643
0.024329666666679;0.0260275000000009 0.0090498333333361
0.026003333333343 -0.0187505000000015 0.0319840000000019 -
0.018999833333350 -0.020258499999994 -0.0038086666666683 -
0.0066648333333344 0.040663666666643 -0.14784183333342
0.082595833333377;0.066705833333347 0.016952499999995
0.0096114999999994 -0.018554166666682 -0.031065000000034 -
0.0125111666666671 -0.025995166666674 -0.0065701666666680 -
0.0376463333333372 0.024329666666679 0.082595833333377 -
0.067853333333320];

```

```

number_of_electrode=12;
%% Multiple input
files = dir('*anc');
%% Eigenvalues_SD matrix
Eigenvalues_SD_matrix=zeros(length(files),number_of_electrode);
%% Eigenvalues_mean matrix
Eigenvalues_mean_matrix=zeros(length(files),number_of_electrode);
%%
for i_files=1:length(files)
    fprintf('Running file %s\n',files(i_files).name)

```

```

fileID = fopen(files(i_files).name); data = textscan(fileID, '%f %f
%f %f %f %f %f %f %f %f');
fclose(fileID);
N=length(data{1,1})/11;
matrix1=horzcat([data{1,1}],[data{1,2};[nan]],[data{1,3};[nan]],[data{
1,4};[nan]],[data{1,5};[nan]],[data{1,6};[nan]],[data{1,7};[nan]],[dat
a{1,8};[nan]],[data{1,9};[nan]],[data{1,10};[nan]],[data{1,11};[nan]]);
;
matrix=zeros(12,12,N);
for i=[1:12]
    for j=[i+1:12]
        matrix(i,j,:)=matrix1(i:11:i+(N-1)*11,j-i);
        matrix(j,i,:)=matrix(i,j,:);
    end
end
for k=[1:N]
    matrix(:,:,k)=matrix(:,:,k)-diag(sum(matrix(:,:,k),2));
%diagonal term
    matrix(:,:,:,k)=(matrix(:,:,:,k)-calibration_air)./(calibration_water-
calibration_air); %calibration
end
matrix_mean=mean(matrix,3);
eigenvalues_mean=transpose(eig(matrix_mean));
matrix_SD=std(matrix,0,3);
eigenvalues_SD=transpose(eig(matrix_SD));

Eigenvalues_SD_matrix(i_files,:)=eigenvalues_SD;
Eigenvalues_mean_matrix(i_files,:)=eigenvalues_mean;
Eigenvalues_CopyMeanRE = horzcat(Eigenvalues_mean_matrix,
Eigenvalues_SD_matrix); %copy excel

end

```

Annex 4: < Eigenvalues calculating using MATLAB code in Annex 3. The first table are the eigenvalues of the mean matrix. The second are from the standard deviation matrix.>

Sam ple	Mean											
	1	2	3	4	5	6	7	8	9	10	11	12
#1	- 0,085 69	- 0,071 69	- 0,049 27	- 0,025 19	- 0,007 79	0,004 997	0,020 663	0,024 642	0,035 611	0,050 162	0,096 01	11,72556 869
#2	- 0,781 58	- 0,640 85	- 0,624 55	- 0,524 67	- 0,477 93	- 0,448 91	- 0,254 35	0,040 777	0,397 84	0,799 687	1,596 206	7,081661 216
#3	- 1,430 25	- 1,231 51	- 0,862 37	- 0,712 34	- 0,578 09	- 0,152 86	- 0,063 22	0,541 539	0,570 363	1,000 725	1,462 47	3,964613 468
#4	- 1,051 16	- 0,980 18	- 0,786 29	- 0,255 23	- 0,107 12	- 0,056 36	- 0,011 89	0,094 551	0,102 97	0,143 875	0,417 518	4,661234 3
#5	- 0,899 49	- 0,860 33	- 0,721 81	- 0,694 36	- 0,081 4	- 0,069 68	- 0,014 02	0,028 261	0,062 717	0,104 468	0,131 599	5,520028 648
#6	- 0,940 91	- 0,750 06	- 0,626 48	- 0,587 32	- 0,554 91	- 0,031 09	- 0,016 93	0,010 009	0,021 936	0,054 073	0,286 55	6,964043 921
#7	- 0,815 12	- 0,755 77	- 0,620 2	- 0,590 99	- 0,549 19	- 0,070 55	- 0,041 34	0,006 641	0,045 926	0,086 962	0,184 267	7,138680 405
#8	- 0,880 15	- 0,749 11	- 0,619 02	- 0,586 03	- 0,544 94	- 0,045 21	- 0,020 11	0,002 723	0,030 111	0,065 334	0,230 673	6,985641 333
#9	- 1,040 12	- 0,832 8	- 0,701 85	- 0,662 63	- 0,067 93	- 0,045 36	- 0,028 95	0,008 949	0,065 118	0,077 753	0,288 556	5,930062 797
#10	- 0,921 19	- 0,838 87	- 0,721 37	- 0,642 78	- 0,089 27	- 0,068 48	- 0,018 01	0,032 958	0,066 36	0,101 448	0,122 103	5,501772 913
#11	- 1,041 63	- 0,997 09	- 0,791 37	- 0,260 8	- 0,073 57	- 0,033 71	- 0,007 38	0,059 741	0,075 127	0,137 618	0,453 363	4,623827 81
#12	- 1,316 48	- 1,102 46	- 0,824 35	- 0,473 1	- 0,347 58	- 0,143 58	- 0,019 31	0,290 12	0,365 392	0,534 822	1,139 838	4,201241 099
#13	- 1,439 55	- 1,245 19	- 0,871 88	- 0,733 26	- 0,602 65	- 0,151 29	- 0,065 2	0,568 555	0,597 066	1,046 548	1,487 861	3,934391 489

#14	-	-	-	-	-	-	-	0,614	0,660	1,227	1,698	3,722281
	1,522	1,337	0,940	0,808	0,602	0,124	0,052	695	72	146	451	444
03	41	73	64	53	3	02						
#15	-	-	-	-	-	-	-	0,033	0,063	0,124	7,741692	
	0,859	0,661	0,604	0,548	0,498	0,205	0,055	0,009	472	593	866	966
71	84	02	39	67	52	91	6					
#16	-	-	-	-	-	-	-	0,067	0,257	0,811	7,721441	
	0,633	0,606	0,486	0,475	0,442	0,261	0,149	0,078	018	039	58	482
91	5	26	87	6	95	66	9					
#17	-	-	-	-	-	-	-	0,238	0,528	1,225	7,843715	
	0,600	0,561	0,498	0,443	0,431	0,415	0,351	0,056	409	115	799	391
99	1	24	43	93	07	78	02					
#18	-	-	-	-	-	-	-	0,294	0,786	1,549	9,036720	
	0,761	0,548	0,403	0,374	0,312	0,288	0,267	0,040	434	396	069	346
57	35	71	79	65	38	84	21					
#19	-	-	-	-	-	-	-	0,310	0,685	1,449	8,085435	
	0,687	0,526	0,510	0,473	0,404	0,388	0,337	0,040	234	811	542	656
57	61	65	13	3	69	07	26					
#20	-	-	-	-	-	-	-	0,027	0,399	0,822	1,593	7,291654
	0,792	0,645	0,610	0,521	0,477	0,448	0,290	238	266	759	014	306
9	85	65	02	43	95	56						
#21	-	-	-	-	-	-	-	0,071	0,457	0,867	1,670	6,608724
	0,808	0,686	0,661	0,576	0,536	0,506	0,268	38	808	389	004	464
02	73	35	01	2	26	78						
#22	-	-	-	-	-	-	-	0,080	0,442	0,837	1,592	6,292272
	0,745	0,731	0,633	0,594	0,564	0,538	0,281	091	521	285	649	89
1	75	87	38	82	14	11						
#23	-	-	-	-	-	-	-	0,101	0,462	0,894	1,630	6,197053
	0,786	0,778	0,659	0,617	0,571	0,531	0,299	954	644	935	054	937
58	11	25	88	15	88	91						
#24	-	-	-	-	-	-	-	0,095	0,223	0,358	8,270202	
	0,765	0,653	0,529	0,487	0,452	0,339	0,096	0,042	365	997	774	358
34	6	09	39	48	16	78	4					
#25	-	-	-	-	-	-	-	0,012	0,214	0,367	0,788	6,459017
	0,797	0,708	0,596	0,560	0,325	0,250	0,112	351	191	876	158	692
24	08	95	75	48	35	06						
#26	-	-	-	-	-	-	-	0,059	0,265	0,452	0,719	5,736028
	0,835	0,795	0,678	0,653	0,388	0,316	0,118	225	457	03	895	437
95	15	53	27	15	91	05						
#27	-	-	-	-	-	-	-	0,041	0,264	0,452	0,673	5,969538
	0,811	0,769	0,654	0,630	0,399	0,324	0,117	058	809	475	579	188
68	65	75	57	68	43	73						
#28	-	-	-	-	-	-	-	0,123	0,151	0,216	0,591	4,898293
	1,131	0,922	0,766	0,496	0,148	0,083	0,012	269	604	886	31	248
05	94	79	33	17	68	06						
#29	-	-	-	-	-	-	-	0,128	0,147	0,247	0,723	4,752036
	1,128	0,995	0,782	0,489	0,137	0,085	0,004	034	659	095	678	423
19	43	71	82	59	38	73						

#30	- 1,162 74	- 1,045 55	- 0,793 48	- 0,510 67	- 0,240 17	- 0,129 32	- 0,017 54	0,200 27	0,240 08	0,363 889	0,869 201	4,649505 613
#31	- 1,180 25	- 1,087 74	- 0,799 83	- 0,513 29	- 0,263 92	- 0,129 15	- -0,018	0,207 693	0,281 434	0,397 194	0,947 98	4,573796 658
#32	- 1,227 08	- 1,127 76	- 0,807 99	- 0,570 88	- 0,384 48	- 0,171 81	- 0,042 34	0,306 569	0,377 093	0,578 851	1,091 774	4,485253 137
#33	- 1,260 94	- 1,157 9	- 0,813 61	- 0,598 08	- 0,438 37	- 0,184 55	- 0,048 01	0,361 256	0,418 289	0,670 268	1,174 12	4,408798 53
#34	- 1,305 61	- 1,101 78	- 0,823 12	- 0,467 7	- 0,340 99	- 0,142 39	- 0,018 7	0,283 318	0,355 956	0,517 598	1,122 846	4,229169 674
#35	- 1,250 66	- 1,065 91	- 0,819 21	- 0,417 69	- 0,242 15	- -0,11	- 0,011 66	0,204 607	0,264 684	0,404 076	0,996 021	4,284414 376
#36	- 1,194 59	- 1,040 74	- 0,815 26	- 0,379 89	- 0,225 72	- 0,105 51	- 0,008 82	0,185 355	0,240 806	0,331 987	0,874 441	4,355246 482
#37	- 1,130 68	- 1,025 25	- 0,809 54	- 0,337 71	- 0,160 16	- 0,075 74	- 0,004 82	0,125 012	0,181 589	0,244 902	0,733 242	4,435831 094
#38	- 1,082 79	- 1,023 12	- 0,802 28	- 0,327 4	- 0,155 09	- 0,075 44	- 0,008 72	0,129 443	0,159 359	0,217 246	0,640 144	4,522917 063
#39	- 1,051 88	- 0,981 43	- 0,786 67	- 0,266 35	- 0,102 67	- 0,054 33	- 0,006 38	0,088 605	0,104 558	0,133 826	0,429 803	4,669765 458
#40	- 1,042 19	- 0,977 13	- 0,802 96	- 0,068 94	- 0,022 5	- 0,009 22	- 0,001 687	0,018 915	0,028 976	0,034 068	0,293 847	4,495212 747
#41	- 1,114 24	- 0,932 47	- 0,814 67	- 0,108 46	- 0,027 04	- 0,007 66	- 0,004 34	0,024 984	0,034 527	0,082 898	0,443 259	4,344272 16
#42	- 1,179 79	- 0,931 19	- 0,809 65	- 0,184 12	- 0,087 5	- 0,033 44	- 0,006 71	0,065 019	0,103 71	0,173 669	0,611 36	4,240951 098
#43	- 1,238 25	- 0,968 08	- 0,810 2	- 0,271 51	- 0,143 89	- 0,065 03	- 0,005 01	0,129 026	0,162 311	0,264 503	0,798 751	4,181954 653
#44	- 1,282 68	- 0,997 92	- 0,814 59	- 0,319 63	- 0,186 89	- 0,075 98	- 0,011 32	0,171 931	0,201 58	0,342 231	0,913 728	4,135878 047
#45	- 1,336 19	- 1,039 36	- 0,815 65	- 0,358 88	- 0,243 22	- 0,095 85	- 0,007 78	0,207 313	0,272 725	0,415 105	1,050 346	4,065924 567

#46	-	-	-	-	-	-	-	0,277	0,346	0,532	1,168	4,017782
	1,375	1,084	0,822	0,425	0,316	0,113	0,014	632	365	01	386	125
	55	9	12	73	55	91	11					
#47	-	-	-	-	-	-	-	0,330	0,404	0,618	1,225	3,983268
	1,400	1,108	0,827	0,468	0,377	0,126	0,019	104	717	06	408	344
	33	01	82	5	41	49	55					
#48	-	-1,274	-	-	-	-0,017	0,014	0,110	0,151	0,196	0,926	3,130623
	1,343		0,261	0,143	0,116		387	465	712	693	611	187
	31		3	67	39							
#49	-	-	-	-	-	-	0,032	0,369	0,418	0,815	1,604	2,928215
	1,580	1,404	0,737	0,345	0,315	0,004	433	524	257	788	612	352
	59	22	6	38	88	48						
#50	-	-	-	-	-	-	0,007	0,028	0,069	0,079	0,167	3,273333
	1,062	0,907	0,264	0,062	0,052	0,015	102	569	68	329	838	25
	16	8	88	87	23	31						
#51	-	-	-	-	-	-	-	0,001	0,004	0,013	0,096	5,327623
	1,169	0,846	0,741	0,514	0,005	0,003	0,001	845	691	579	226	623
	23	5	88	52	89	45	08					
#52	-	-	-	-	-	-	0,000	0,003	0,006	0,026	0,116	5,463244
	1,000	0,915	0,743	0,729	0,012	0,002	206	503	691	899	169	325
	31	5	28	81	18	77						
#53	-	-	-	-	-	-	0,000	0,003	0,008	0,034	0,342	6,210563
	1,090	0,826	0,679	0,640	0,201	0,012	845	485	336	002	791	515
	71	99	3	32	14	89						
#54	-	-	-	-	-	-	0,000	0,002	0,008	0,036	0,314	6,081062
	1,075	0,827	0,688	0,650	0,148	0,009	128	843	315	191	168	517
	53	68	98	62	58	32						
#55	-	-	-	-	-	-	0,000	0,002	0,007	0,042	0,278	5,922615
	1,057	0,832	0,702	0,664	0,092	0,003	142	049	292	939	857	617
	94	79	96	16	54	9						
#56	-	-	-	-	-	-	0,001	0,001	0,006	0,053	0,262	5,797812
	1,051	0,839	0,717	0,675	0,057	0,000	069	986	989	413	46	882
	63	71	03	95	23	7						
#57	-	-	-	-	-	-	0,001	0,005	0,006	0,070	0,224	5,649564
	1,031	0,861	0,739	0,694	0,029	0,001	01	317	813	687	029	133
	88	48	68	24	69	39						
#58	-	-	-	-	-	-	0,000	0,005	0,007	0,091	0,167	5,559984
	1,024	0,906	0,767	0,712	0,019	0,001	727	397	925	702	426	926
	32	26	66	91	6	55						
#59	-	-	-	-	-	-	0,000	0,005	0,007	0,093	0,163	5,555788
	1,024	0,910	0,769	0,714	0,019	0,001	908	057	88	288	333	953
	83	42	27	23	21	43						
#60	-	-	-	-	-	-	0,000	0,005	0,007	0,088	0,149	5,537077
	1,029	0,924	0,777	0,720	0,015	0,001	671	016	206	962	817	266
	63	86	37	65	87	97						
#61	-	-	-	-	-	-	0,000	0,004	0,006	0,076	0,138	5,531016
	1,028	0,924	0,779	0,724	0,013	0,002	578	432	909	17	636	365
	75	69	68	49	58	34						

#62	- 1,024 35	- 0,919 53	- 0,781 19	- 0,728 07	- 0,011 36	- 0,002 8	0,000 222	0,004 098	0,005 881	0,057 337	0,125 242	5,526236 941
#63	- 0,992 5	- 0,932 48	- 0,774 07	- 0,731 38	- 0,009 43	- 0,003 34	7,58E- 05	0,004 137	0,005 194	0,039 931	0,117 186	5,507135 49
#64	- 1,053 94	- 0,883 24	- 0,739 52	- 0,698 03	- 0,009 16	- 0,003 17	- 0,000 2	0,003 879	0,004 171	0,023 472	0,121 701	5,419249 068
#65	- 0,839 46	- 0,781 7	- 0,681 48	- 0,653 17	- 0,417 93	- 0,347 99	- 0,129 75	0,059 715	0,275 109	0,486 922	0,769 873	5,718808 038
#66	- 0,821 22	- 0,783 36	- 0,665 75	- 0,642 42	- 0,371 43	- 0,298 38	- 0,104 62	0,046 946	0,258 476	0,419 486	0,626 332	5,840353 002
#67	- 0,746 87	- 0,695 59	- 0,587 86	- 0,556 35	- 0,292 7	- 0,225 56	- 0,150 63	- 0,013 29	0,109 084	0,253 586	0,323 641	6,755890 355
#68	- 0,732 1	- 0,706 94	- 0,540 4	- 0,529 7	- 0,478 32	- 0,299 54	- 0,044 86	- 0,001 29	0,045 429	0,058 376	0,104 225	8,123408 204
#69	- 0,900 31	- 0,719 67	- 0,598 48	- 0,527 41	- 0,486 6	- 0,374 29	- 0,033 18	0,017 25	0,031 682	0,146 586	0,169 705	8,287484 143
#70	- 0,924 84	- 0,656 69	- 0,526 12	- 0,488 33	- 0,451 58	- 0,378 84	- 0,025 31	0,000 651	0,026 585	0,135 326	0,255 268	8,440465 382
#71	- 0,851 83	- 0,631 73	- 0,493 28	- 0,455 37	- 0,419 78	- 0,338 35	- 0,044 98	- 0,002 39	0,027 425	0,144 475	0,238 18	8,696007 807
#72	- 0,730 76	- 0,596 33	- 0,462 42	- 0,431 52	- 0,398 34	- 0,272 42	- 0,130 31	0,005 607	0,102 211	0,178 195	0,273 95	8,706849 958
#73	- 0,682 76	- 0,628 44	- 0,577 74	- 0,528 61	- 0,493 35	- 0,464 9	- 0,232 1	0,063 803	0,398 892	0,749 877	1,601 339	6,795358
#74	- 0,678 37	- 0,648 39	- 0,579 11	- 0,540 83	- 0,511 13	- 0,482 15	- 0,238 91	0,073 206	0,408 299	0,756 424	1,625 492	6,618844
#75	- 0,659 04	- 0,633 6	- 0,577 18	- 0,522 06	- 0,504 97	- 0,476 26	- 0,216 82	0,068 179	0,389 66	0,716 982	1,582 881	6,625996
#76	- 0,677 19	- 0,644 14	- 0,592 98	- 0,539 85	- 0,520 91	- 0,490 07	- 0,212 63	0,066 949	0,395 318	0,708 844	1,542 798	6,437301
#77	- 0,682 76	- 0,648 73	- 0,591 68	- 0,543 59	- 0,522 9	- 0,487 09	- 0,204 19	0,065 737	0,386 14	0,698 76	1,502 874	6,416767

#78	-	-	-	-	-	-	-	0,195	0,428	0,760	0,983	4,870247
	0,889	0,828	0,746	0,642	0,563	0,320	0,129	79	283	664	846	
	98	73	64	49	68	49	72					
#79	-	-	-	-	-	-	-	0,309	0,514	0,944	1,021	5,110629
	1,137	0,884	0,791	0,738	0,694	0,355	0,182	11	237	513	655	
	19	05	93	13	02	16	16					
#80	-	-	-	-	-	-	-	0,314	0,466	0,833	0,963	5,080559
	1,179	0,892	0,775	0,728	0,617	0,311	0,156	003	225	767	259	
	98	5	52	9	35	46	16					
#81	-	-	-	-	-	-	-	0,321	0,451	0,777	0,988	4,829007
	1,167	0,982	0,777	0,672	0,558	0,253	0,127	52	63	606	644	
	25	05	27	51	38	61	76					
#82	-	-	-	-	-	-	-	0,312	0,413	0,673	0,996	4,746572
	1,184	1,030	0,783	0,645	0,471	0,218	0,092	961	978	465	751	
	89	65	9	67	37	04	75					
#83	-	-	-	-	-0,463	-	-	0,343	0,418	0,676	1,086	4,608058
	1,225	1,099	0,795	0,632		0,203	0,075	33	503	679	467	
	01	02	25	17		11	63					
#84	-	-	-	-	-	-	-	0,431	0,494	0,822	1,260	4,339582
	1,295	1,175	0,818	0,662	0,532	0,192	0,075	337	383	776	824	
	84	32	57	77	28	62	44					
#85	-	-	-	-	-	-	-	0,022	0,065	0,105	0,123	5,475683
	0,985	0,871	0,727	0,689	0,068	0,051	0,006	572	564	124	384	
	81	16	31	41	88	69	93					
#86	-	-	-	-	-	-	-	0,003	0,004	0,044	0,137	5,45813
	1,028	0,866	0,727	0,686	0,006	0,003	0,000	84	939	552	064	
	45	02	56	77	85	99	54					
#87	-	-	-	-	-	-	-	0,002	0,012	0,055	0,280	5,359696
	1,061	0,794	0,729	0,586	0,007	0,003	0,000	517	826	969	44	
	93	15	11	71	45	41	52					
#88	-	-	-	-	-	-	-	0,253	0,337	0,567	0,881	5,187778
	1,211	0,888	0,781	0,717	0,400	0,220	0,091	447	195	042	815	
	3	23	14	42	43	94	5					
#89	-	-	-	-	-	-	-	0,349	0,435	0,763	1,068	5,035394
	1,238	1,000	0,783	0,735	0,531	0,263	0,120	357	547	072	792	
	98	22	21	86	28	84	32					
#90	-	-	-	-	-	-	-	0,421	0,504	0,932	1,244	4,895862
	1,260	1,103	0,813	0,762	0,613	0,273	0,151	824	754	658	856	
	4	52	2	01	9	06	37					
#91	-	-	-	-	-	-	-	0,242	0,55	1,226	7,654625	
	0,624	0,595	0,522	0,465	0,445	0,435	0,352	0,045	403		563	587
	21	81	3	37	76	44	99	13				
#92	-	-	-	-	-	-	-	0,019	0,313	0,621	1,278	6,806524
	0,752	0,656	0,558	0,531	0,503	0,431	0,215	752	651	395	843	587
	28	26	17	7	98	27	98					
#93	-	-	-	-	-	-	-	0,065	0,385	0,665	1,274	6,046397
	0,784	0,724	0,620	0,590	0,568	0,469	0,180	703	966	645	874	279
	97	51	28	23	53	29	58					

#94	- 0,781 1	- 0,717 02	- 0,630 41	- 0,616 51	- 0,590 56	- 0,505 88	- 0,223 44	0,072 166	0,381 174	0,700 37	1,219 294	5,940636 292
#95	- 0,820 11	- 0,747 27	- 0,659 62	- 0,640 2	- 0,618 98	- 0,518 59	- 0,235 21	0,078 779	0,396 272	0,732 627	1,065 823	5,844283 949
#96	- 0,962 81	- 0,883 75	- 0,747 24	- 0,730 51	- 0,679 8	- 0,475 34	- 0,264 91	0,187 328	0,483 776	0,959 649	1,067 408	5,701674 042
#97	- 1,109 42	- 0,999 34	- 0,812 64	- 0,750 37	- 0,686 63	- 0,472 41	- 0,280 21	0,301 117	0,535 202	1,130 561	1,157 106	5,679914 452
#98	- 0,865 17	- 0,664 27	- 0,616 37	- 0,554 77	- 0,506 81	- 0,131 61	- 0,044 22	- 0,004 52	0,026 805	0,046 237	0,118 094	7,603595 455
#99	- 0,811 16	- 0,750 6	- 0,628 65	- 0,593 55	- 0,359 89	- 0,173 86	- 0,115 04	0,016 899	0,125 514	0,208 448	0,233 976	6,683109 148
#100	- 0,846 98	- 0,805 42	- 0,679 26	- 0,664 38	- 0,299 91	- 0,236 43	- 0,085 98	0,052 112	0,197 582	0,355 12	0,379 336	5,836619 945
#101	- 0,886 93	- 0,821 2	- 0,707 49	- 0,677 8	- 0,327 35	- 0,275 19	- 0,105 54	0,058 107	0,225 355	0,388 606	0,417 978	5,579081 524
#102	- 0,921 75	- 0,821 09	- 0,711 93	- 0,655 97	- 0,182 87	- -0,134 49	- 0,056 49	0,066 477	0,126 537	0,223 073	0,255 628	5,561920 695
#103	- 1,019 47	- 0,806 22	- 0,721 46	- 0,607 53	- 0,150 16	- 0,095 58	- 0,040 77	0,090 943	0,114 89	0,185 648	0,284 632	5,433381 061
#104	- 1,082 77	- 0,808 54	- 0,729 8	- 0,561 53	- 0,068 23	- 0,037 48	- 0,008 6	0,052 846	0,073 537	0,094 32	0,298 977	5,301961 032
#105	- 1,127 99	- 0,922 34	- 0,766 95	- 0,494 38	- 0,125 73	- 0,073 4	- 0,004 3	0,109 292	0,135 258	0,188 031	0,586 195	4,897921 937
#106	- 1,181 18	- 1,063 85	- 0,795 8	- 0,534 67	- 0,283 43	- 0,134 4	- 0,029 15	0,224 069	0,280 576	0,418 857	0,931 582	4,621053 145
#107	- 1,321 26	-1,225 56	- 0,825 66	- 0,714 92	- 0,571 42	- 0,192 93	- 0,082 93	0,482 739	0,531 788	0,923 977	1,346 693	4,282283 519
#108	- 1,282 91	- 1,277 63	- 0,838 29	- 0,802 02	- 0,692 48	- 0,236 65	- 0,139 61	0,538 866	0,603 7	1,107 458	1,427 89	4,473820 704
#109	- 1,224 4	- 1,033 36	- 0,781 33	- 0,691 82	- 0,455 41	- 0,227 8	- 0,077 65	0,326 644	0,400 104	0,649 9	1,039 867	4,854073 146

#110	-	-	-	-	-	-	-	0,206	0,285	0,439	0,787	5,127250	
	1,176	0,883	0,756	0,703	0,314	0,165	0,069	131	786	943	824	838	
	24	16	54	34	77	87	35						
#111	-	-	-	-	-	-	-	0,151	0,212	0,344	0,566	5,405915	
	1,058	0,804	0,747	0,718	0,257	0,152	0,071	866	55	891	101	243	
	83	29	37	01	39	04	57						
#112	-	-	-	-	-	-	-	0,145	0,196	0,337	0,474	5,557838	
	0,990	0,825	0,716	0,699	0,271	0,170	0,079	545	788	314	83	551	
	84	15	49	92	56	18	36						
#113	-	-	-	-	-	-	-	0,139	0,330	0,615	0,665	5,578297	
	0,949	0,825	0,710	0,689	0,505	0,343	0,179	229	549	54	183	351	
	97	8	59	65	31	73	59						
#114	-	-	-	-	-	-	-	0,101	0,313	0,580	0,624	5,497047	
	0,944	0,791	0,707	0,631	0,483	0,352	0,167	681	989	668	794	564	
	73	99	8	52	58	06	45						
#115	-	-	-	-	-	-	-	0,064	0,288	0,508	0,558	5,571591	
	0,911	0,813	0,702	0,616	0,426	0,355	0,145	57	805	328	287	475	
	38	09	98	16	67	6	15						
#116	-	-	-	-	-	-	-	0,056	0,238	0,422	0,549	5,591566	
	0,888	0,806	0,692	0,609	0,364	0,298	0,122	735	595	883	059	072	
	01	64	44	65	5	36	21						
#117	-	-	-	-	-	-	-	-	0,054	0,199	0,258	7,452812	
	0,724	0,680	0,560	0,528	0,408	0,191	0,147	0,072	172	062	243	69	
	68	74	87	16	71	72	14	07					
#118	-	-	-	-	-	-	-	0,073	0,440	0,831	1,612	6,445308	
	0,772	0,685	0,651	0,572	0,532	0,501	0,253	831	99	844	799	178	
	83	85	94	27	4	13	68						
#119	-	-0,701	-	-	-	-	-	-	0,002	0,009	0,056	0,097	8,101738
	0,738		0,548	0,531	0,482	0,305	0,013	188	602	78	548	596	
	68		17	95	29	4	66						
#120	-	-	-	-	-	-	-	-	0,052	0,086	0,139	8,037497	
	0,739	0,671	0,547	0,528	0,478	0,265	0,078	0,019	962	698	013	276	
	07	86	34	56	81	63	41	75					
#121	-	-	-	-	-	-	-	-	0,056	0,147	0,174	7,980744	
	0,739	0,667	0,551	0,529	0,481	0,248	0,126	0,042	21	35	489	372	
	44	82	41	83	04	11	76	21					
#122	-	-	-	-	-	-	-	-	0,009	0,182	0,365	0,437	6,384221
	0,777	0,737	0,621	0,598	0,342	0,273	0,141	46	853	916	133	051	
	3	86	97	92	79	06	86						
#123	-	-	-	-	-	-	-	-	0,060	0,312	0,537	0,607	5,655674
	0,861	0,820	0,695	0,659	0,466	0,392	0,158	125	949	428	059	586	
	95	99	32	98	53	47	26						
#124	-	-	-	-	-	-	-	-	0,105	0,356	0,663	0,701	5,521090
	0,967	0,810	0,709	0,657	0,538	0,388	0,183	669	006	494	929	198	
	51	06	77	86	78	81	69						
#125	-	-	-	-	-	-	-	-	0,124	0,284	0,527	0,577	5,579600
	0,933	0,805	0,704	0,678	0,431	0,299	0,149	281	806	999	964	888	
	57	9	43	68	45	22	11						

#126	- 1,000 38	- 0,832 42	- 0,720 17	- 0,702 7	- 0,262 77	- 0,164 15	- 0,077 5	0,141 414	0,185 312	0,339 914	0,495 722	5,558839 535
#127	- 1,058 45	- 0,808 78	- 0,731 04	- 0,716 04	- 0,145 03	- 0,092 51	- 0,024 2	0,080 9	0,124 891	0,229 043	0,494 541	5,453983 329
#128	- 1,168 33	- 0,894 23	- 0,760 02	- 0,696 76	- 0,329 2	- 0,187 35	- 0,061 88	0,225 662	0,290 595	0,457 797	0,799 903	5,102522 345
#129	- 1,260 03	- 1,149 96	- 0,812 7	- 0,597 69	- 0,434 6	- 0,181 89	- 0,050 62	0,352 547	0,420 416	0,664 771	1,171 832	4,406711 97
#130	- 1,166 45	- 1,044 97	- 0,793 56	- 0,516 78	- 0,223 18	- 0,116 95	- 0,018 63	0,186 215	0,229 635	0,354 789	0,881 569	4,649707 748
#131	- 0,841 66	- 0,814 69	- 0,683 1	- 0,665 59	- 0,313 85	- 0,252 88	- 0,084 85	0,047 715	0,220 325	0,369 347	0,399 647	5,827012 914
#132	- 0,855 58	- 0,665 84	- 0,615 62	- 0,557 46	- 0,509 56	- 0,114 35	- 0,055 03	0,026 036	0,063 541	0,117 785	7,588960 803	
#133	- 1,130 57	- 1,015 12	- 0,809 57	- 0,332 66	- 0,120 54	- 0,062 68	- -0,007 801	0,109 408	0,135 232	0,232 0,725	4,425232 477	484
#134	- 1,071 46	- 0,881 89	- 0,777 14	- 0,739 94	- 0,634 16	- 0,334 68	- 0,159 4	0,288 17	0,488 104	0,869 59	0,976 069	4,970853
#135	- 1,225 05	- 0,900 5	- 0,785 01	- 0,720 64	- 0,487 62	- 0,258 02	- 0,114 16	0,287 171	0,394 891	0,680 795	0,939 087	5,162016
#136	- 1,225 5	- 0,990 94	- 0,777 18	- 0,728 96	- 0,476 75	- 0,241 99	- 0,108 84	0,315 058	0,403 743	0,695 978	1,035 721	5,036181
#137	- 1,260 28	- 1,107 52	- 0,815 88	- 0,762 64	- 0,639 6	- 0,279 73	- 0,157 83	0,434 53	0,522 098	0,962 672	1,259 716	4,883081

Sam ple	SD											
	1	2	3	4	5	6	7	8	9	10	11	12
#1	- 0,024 73	- 0,000 54	- 0,000 51	- 0,000 39	- 0,000 14	-2,8E- 05	0,000 179	0,000 525	0,000 846	0,000 971	0,002 071	0,032688 823
#2	- 0,975 87	- 0,314 54	- 0,184 86	- 0,096 24	0,011 2	0,038 736	0,058 964	0,080 257	0,157 207	0,232 304	0,264 335	4,009897 2

#3	- 0,383 45	- 0,371 38	- 0,119 37	- 0,093 31	- 0,038 13	0,009 36	0,040 013	0,105 494	0,129 451	0,173 294	0,217 971	0,718891 335
#4	- 0,398 75	- 0,276 36	- 0,057 26	- 0,015 06	- 0,009 58	0,003 294	0,007 968	0,019 559	0,040 988	0,059 47	0,226 466	0,698767 671
#5	- 0,289 57	- 0,216 12	- 0,003 05	- 0,001 61	- 0,000 34	0,001 001	0,004 599	0,017 119	0,017 838	0,059 716	0,125 882	0,498188 965
#6	- 0,154 17	- 0,048 94	- 0,001 13	- 0,000 61	- 0,000 35	0,000 255	0,001 377	0,007 186	0,008 307	0,009 135	0,049 082	0,234987 737
#7	- 0,126 79	- 0,020 32	- 0,000 91	- 0,000 52	- 0,000 36	0,000 254	0,001 434	0,004 343	0,005 703	0,006 638	0,023 274	0,181074 767
#8	- 0,245 25	- 0,056 5	- 0,001 63	- 0,001 1	- 0,000 51	0,000 467	0,002 401	0,010 703	0,011 413	0,012 22	0,063 977	0,356124 687
#9	- 0,412 91	- 0,060 9	- 0,003 97	- 0,002 1	- 0,000 18	0,002 784	0,006 718	0,022 361	0,023 054	0,025 555	0,107 142	0,544978 374
#10	- 0,302 74	- 0,245 43	- 0,007 48	- 0,004 81	0,000 177	0,005 558	0,010 615	0,017 411	0,018 77	0,064 606	0,141 38	0,527078 886
#11	- 0,412 02	- 0,293 79	- 0,058 6	- 0,004 63	- 0,003 1	0,001 05	0,001 973	0,008 9	0,042 887	0,060 385	0,236 872	0,736164 53
#12	- 0,395 27	- 0,385 86	- 0,103 35	- 0,067 73	- 0,033 85	0,009 547	0,032 531	0,067 856	0,107 834	0,111 844	0,264 404	0,773449 193
#13	- 0,396 44	- 0,385 68	- 0,120 25	- 0,095 12	- 0,038 02	0,010 533	0,038 292	0,104 817	0,136 143	0,181 671	0,219 66	0,746575 247
#14	- 0,388 31	- 0,364 31	- 0,132 48	- 0,112 62	- 0,038 2	0,006 956	0,039 307	0,097 944	0,153 243	0,171 862	0,265 085	0,683346 312
#15	- 0,096 41	- 0,009 8	- 0,001 5	- 0,000 97	0,000 266	0,000 534	0,003 378	0,004 739	0,004 768	0,004 813	0,012 907	0,122543 685
#16	- 0,812 48	- 0,181 06	- 0,066 47	- 0,035 8	- 0,018 16	0,021 845	0,025 924	0,040 327	0,055 983	0,065 04	0,110 107	3,369375 804
#17	- 1,056 51	- 0,212 06	- 0,114 59	- 0,026 39	- 0,029 336	0,040 827	0,055 478	0,075 421	0,090 107	0,120 278	0,154 762	3,741240 705
#18	- 1,224 17	- 0,567 98	- 0,204 23	- 0,108 86	0,005 341	0,032 983	0,061 077	0,093 783	0,182 102	0,349 123	0,448 232	4,051475 106

#19	- 1,164 08	- 0,358 03	- 0,117 38	- 0,072 69	0,022 65	0,059 977	0,068 285	0,098 886	0,122 17	0,194 367	0,270 302	4,077110 772
#20	- 1,029 98	- 0,373 09	- 0,180 49	- 0,096 46	0,018 81	0,056 419	0,087 253	0,111 998	0,151 172	0,251 569	0,287 933	4,062586 75
#21	- 0,996 91	- 0,329 52	- 0,161 76	- 0,076 5	0,036 521	0,059 483	0,103 252	0,125 066	0,144 908	0,239 395	0,260 875	4,021197 652
#22	- 0,987 2	- 0,229 18	- 0,088 12	- 0,060 1	0,035 685	0,059 213	0,098 461	0,123 438	0,131 312	0,147 842	0,188 699	3,882164 575
#23	- 0,952 45	- 0,205 74	- 0,080 42	- 0,065 76	0,022 851	0,056 905	0,094 502	0,112 46	0,130 107	0,150 85	0,185 745	3,774309 871
#24	- 0,554 32	- 0,194 54	- 0,060 48	- 0,024 55	- 0,009 99	- 0,001 89	0,008 744	0,025 632	0,028 161	0,089 484	0,119 548	2,133886 685
#25	- 0,941 39	- 0,194 93	- 0,040 14	- 0,000 66	0,011 327	0,012 873	0,038 639	0,048 66	0,089 966	0,098 379	0,226 098	3,338957 842
#26	- 0,777 87	- 0,121 34	- 0,033 35	- 0,021 11	0,005 553	0,017 065	0,051 342	0,070 942	0,081 91	0,143 761	0,151 047	2,448137 844
#27	- 0,960 93	- 0,155 99	- 0,070 74	- 0,042 8	-5,7E- 06	0,016 216	0,075 311	0,079 782	0,097 477	0,137 363	0,261 955	2,510838 726
#28	- 0,453 91	- 0,227 9	- 0,119 06	- 0,042 25	- 0,033 38	0,009 157	0,024 603	0,046 139	0,061 156	0,091 137	0,215 4	0,811883 551
#29	- 0,476 35	- 0,276 59	- 0,118 27	- 0,020 76	- 0,017 42	0,003 4	0,012 022	0,027 945	0,053 577	0,095 792	0,251 457	0,862185
#30	- 0,456 47	- 0,314 33	- 0,152 55	- 0,085 82	- 0,044 7	0,011 371	0,028 166	0,059 234	0,113 775	0,149 577	0,269 543	0,872179 329
#31	- 0,455 83	- 0,324 64	- 0,125 46	- 0,064 7	- 0,047 26	0,007 848	0,032 037	0,060 709	0,096 999	0,122 269	0,273 455	0,856717 204
#32	- 0,461 25	- 0,366 32	- 0,157 32	- 0,112 11	- 0,050 08	0,011 141	0,040 463	0,071 934	0,145 372	0,177 074	0,281 228	0,893500 544
#33	- 0,449 76	- 0,374 18	- 0,135 45	- 0,097 32	- 0,044 46	0,012 639	0,035 534	0,075 329	0,136 847	0,159 04	0,272 327	0,863356 099
#34	- 0,400 44	- 0,383 7	- 0,088 06	- 0,052 61	- 0,031 67	0,010 774	0,025 312	0,061 562	0,092 071	0,098 732	0,263 308	0,779817 337

#35	- 0,414 53	- 0,385 24	- 0,095 68	- 0,048 86	- 0,034 61	0,008 995	0,027 721	0,056 938	0,088 632	0,097 103	0,283 497	0,802768 553
#36	- 0,417 95	- 0,376 46	- 0,079 5	- 0,032 81	- 0,032 02	0,013 491	0,015 145	0,045 397	0,070 862	0,080 054	0,288 209	0,798552 532
#37	- 0,422 91	- 0,357 71	- 0,075 33	- 0,032 22	- 0,013 36	0,006 555	0,012 055	0,037 681	0,052 405	0,078 867	0,280 236	0,793405 51
#38	- 0,424 65	- 0,326 1	- 0,096 01	- 0,037 85	- 0,020 57	0,008 079	0,015 533	0,039 571	0,066 918	0,095 316	0,263 537	0,787560 023
#39	- 0,423 27	- 0,282 61	- 0,061 33	- 0,009 01	- 0,006 05	0,002 526	0,005 596	0,013 407	0,041 533	0,060 59	0,233 55	0,739471 873
#40	- 0,350 13	- 0,299 95	- 0,019 17	- 0,004 26	- 0,001 59	0,000 893	0,001 783	0,006 38	0,027 501	0,042 361	0,218 471	0,633026 246
#41	- 0,354 49	- 0,322 4	- 0,026 47	- 0,010 44	- 0,001 51	0,000 915	0,002 604	0,013 875	0,030 992	0,048 531	0,230 493	0,659517 24
#42	- 0,385 91	- 0,351 17	- 0,038 14	- 0,016 25	- 0,005 84	0,000 721	0,012 017	0,020 463	0,041 224	0,058 191	0,260 594	0,711709 811
#43	- 0,407 77	- 0,371 85	- 0,044 23	- 0,023 18	- 0,018 37	0,003 025	0,018 89	0,032 991	0,049 776	0,066 081	0,278 686	0,751271 407
#44	- 0,400 39	- 0,365 74	- -0,049 0,029	- 0,025 48	- 0,025 15	0,012 823	0,015 439	0,044 918	0,050 977	0,075 579	0,272 017	0,725821 419
#45	- 0,398 42	- 0,371 49	- 0,057 27	- 0,034 77	- 0,027 98	0,010 765	0,020 483	0,046 304	0,062 643	0,098 855	0,255 569	0,738426 983
#46	- 0,385 15	- 0,372 48	- 0,106 61	- 0,077 61	- 0,039 69	0,012 244	0,039 359	0,096 263	0,102 454	0,128 134	0,242 394	0,738503 123
#47	- 0,376 23	- 0,350 99	- 0,092 72	- 0,066 75	- 0,029 73	0,008 531	0,031 229	0,083 207	0,090 726	0,127 619	0,232 72	0,687491 921
#48	- 0,230 99	- 0,199 72	- 0,056 29	- 0,018 56	- 0,008 51	- 0,003 91	0,007 282	0,011 1	0,025 083	0,069 728	0,169 316	0,401442 498
#49	- 0,221 62	- 0,184 91	- 0,076 14	- 0,052 79	- 0,028 62	- 0,006 18	0,015 069	0,037 958	0,066 092	0,101 465	0,204 062	0,306296 12
#50	- 0,444 55	- 0,176 92	- 0,005 18	- 0,003 53	- 0,001 49	0,000 789	0,002 966	0,004 337	0,007 879	0,030 9	0,234 682	0,572792 583

#51	- 0,018 4	- 0,001 23	- 0,000 48	- 0,000 37	- 0,000 34	- 0,000 17	-3,4E- 05	0,000 21	0,000 341	0,001 478	0,002 693	0,022189 944
#52	- 0,052 74	- 0,005 14	- 0,000 62	- 0,000 48	- 0,000 27	- 0,000 17	-4,3E- 05	0,000 136	0,000 588	0,000 662	0,005 83	0,063378 904
#53	- 0,113 04	- 0,014 75	- 0,000 88	- 0,000 63	- 0,000 28	- 0,000 149	0,002 133	0,006 851	0,006 994	0,007 759	0,021 768	0,152343 586
#54	- 0,106 6	- 0,013 14	- 0,000 58	- 0,000 4	- 0,000 14	- 0,000 05	-2,2E- 658	0,001 236	0,006 335	0,006 143	0,020 6	0,142233 478
#55	- 0,194 99	- 0,017 48	- 0,000 66	- 0,000 42	- 0,000 32	- 0,000 1	- 0,000 126	0,002 163	0,010 431	0,012 02	0,032 106	0,254610 619
#56	- 0,238 06	- 0,025 46	- 0,000 75	- 0,000 44	- 0,000 37	- 0,000 06	9,1E- 152	0,002 362	0,012 795	0,014 675	0,045 682	0,309857 697
#57	- 0,222 01	- 0,030 67	- 0,000 6	- 0,000 45	- 0,000 23	- 0,000 05	-3,3E- 953	0,001 059	0,011 944	0,013 124	0,060 161	0,284987 1
#58	- 0,023 8	- 0,001 88	- 0,000 53	- 0,000 27	- 0,000 05	- 0,000 119	-4,6E- 836	0,000 264	0,001 308	0,001 621	0,003 834	0,030502 168
#59	- 0,018 99	- 0,001 52	- 0,000 67	- 0,000 24	- 0,000 2	- 0,000 124	0,000 597	0,001 018	0,001 126	0,001 48	0,003 509	0,024408 432
#60	- 0,009 38	- 0,001 15	- 0,000 49	- 0,000 4	- 0,000 31	- 0,000 17	- 0,000 488	0,000 588	0,000 759	0,001 427	0,002 152	0,012369 367
#61	- 0,013 2	- 0,001 82	- 0,000 32	- 0,000 3	- 0,000 26	- 0,000 17	- 0,000 847	0,000 9	0,000 952	0,001 415	0,003 233	0,016963 689
#62	- 0,010 95	- 0,001 93	- 0,000 49	- 0,000 35	- 0,000 13	- 0,000 105	0,000 3	0,000 597	0,000 774	0,001 259	0,002 971	0,013460 747
#63	- 0,040 37	- 0,007 97	- 0,000 74	- 0,000 35	- 0,000 29	- 0,000 16	- 0,000 11	0,000 727	0,001 124	0,001 562	0,009 219	0,049024 707
#64	- 0,066 72	- 0,008 34	- 0,000 54	- 0,000 36	- 0,000 34	- 0,000 27	- 0,000 16	0,000 66	0,001 231	0,001 831	0,008 663	0,079993 653
#65	- 0,799 34	- 0,086 83	- 0,048 48	- 0,027 76	- 0,001 37	- 0,014 13	0,061 785	0,076 071	0,087 723	0,117 943	0,173 943	2,500349 328
#66	- 0,954 21	- 0,129 28	- 0,079 45	- 0,052 05	- 0,011 873	- 0,033 899	0,075 627	0,081 241	0,099 662	0,143 412	0,240 632	2,437130 61

#67	- 1,070 85	- 0,241 16	- 0,143 53	- 0,069 91	- 0,057 53	0,005 414	0,081 499	0,089 995	0,138 248	0,169 999	0,376 435	2,301314 189
#68	- 0,312 71	- 0,095 31	- 0,002 07	- 0,001 67	0,003 733	0,013 9	0,019 064	0,022 008	0,025 75	0,039 335	0,066 634	0,481037 936
#69	- 0,053 48	- 0,011 29	- 0,000 74	- 0,000 35	0,001 135	0,002 113	0,002 175	0,002 283	0,002 515	0,003 427	0,013 628	0,070209 883
#70	- 0,130 85	- 0,004 82	- 0,001 45	9,96E- 05	0,002 325	0,006 1	0,006 169	0,006 246	0,006 495	0,007 06	0,019 552	0,174591 623
#71	- 0,263 76	- 0,036 81	- 0,002 32	- 0,000 95	0,003 772	0,014 155	0,014 33	0,014 489	0,014 816	0,017 622	0,076 933	0,362727 01
#72	- 0,674 24	- 0,146 03	- 0,025 36	- 0,016 52	- 0,000 35	0,012 929	0,021 76	0,031 976	0,036 429	0,091 352	0,112 861	1,907997 51
#73	- 1,067 09	- 0,340 68	- 0,182 8	- 0,072 49	0,055 891	0,064 44	0,102 838	0,115 174	0,161 712	0,244 424	0,284 126	4,30498
#74	- 1,063 36	- 0,336 6	- 0,172 39	- 0,061 39	0,061 925	0,072 963	0,106 48	0,119 004	0,156 859	0,239 86	0,277 539	4,276222
#75	- 1,064 4	- 0,332 25	- 0,172 84	- 0,062 15	0,059 704	0,069 751	0,106 795	0,119 216	0,160 457	0,245 184	0,274 541	4,290729
#76	- 1,049 59	- 0,290 25	- 0,136 77	- 0,056 36	0,061 326	0,068 8	0,108 104	0,120 681	0,151 24	0,214 808	0,238 937	4,158356
#77	- 1,041 22	- 0,276 51	- 0,127 3	- 0,055 72	0,055 703	0,066 638	0,106 036	0,117 986	0,144 434	0,208 209	0,224 91	4,100184
#78	- 0,544 74	- 0,292 43	- 0,055 18	- 0,050 18	- 0,043 41	- 0,011 77	0,007 789	0,046 787	0,106 999	0,128 863	0,200 683	2,558326
#79	- 0,544 19	- 0,336 78	- 0,262 91	- 0,209 27	- 0,065 91	- 0,034 58	0,039 351	0,095 405	0,168 239	0,336 581	0,376 301	1,378991
#80	- 0,453 41	- 0,339 15	- 0,221 68	- 0,199 76	- 0,077 59	- 0,003 13	0,040 192	0,086 82	0,168 676	0,296 89	0,314 78	1,15183
#81	- 0,483 88	- 0,359 95	- 0,206 08	- 0,205 47	- 0,101 71	- 0,005 49	0,039 391	0,104 026	0,206 026	0,282 111	0,322 872	1,177681
#82	- 0,469 08	- 0,350 41	- 0,206 19	- 0,170 27	- 0,112 31	0,019 223	0,047 725	0,105 344	0,224 699	0,237 939	0,262 979	1,037525

#83	- 0,442 01	- 0,345 36	- 0,192 48	- 0,152 51	- 0,099 41	0,019 94	0,043 825	0,101 143	0,212 358	0,227 764	0,262 76	0,889158
#84	- 0,427 77	- 0,399 19	- 0,139 27	- 0,108 01	- 0,058 11	0,016 248	0,043 469	0,090 597	0,153 459	0,170 383	0,266 215	0,864204
#85	- 0,071 53	- 0,036 04	- 0,001 64	- 0,001 08	- 0,000 13	0,001 12	0,001 434	0,001 959	0,002 239	0,008 31	0,029 505	0,09407
#86	- 0,105 29	- 0,042 73	- 0,000 61	- 0,000 37	- 0,000 23	1,64E- 05	0,000 739	0,001 769	0,004 483	0,007 258	0,039 153	0,146071
#87	- 0,406 14	- 0,248 71	- 0,007 35	- 0,001 77	- 0,000 65	-5,9E- 05	0,003 414	0,028 919	0,039 717	0,059 855	0,107 025	0,741762
#88	- 0,491 46	- 0,337 14	- 0,160 22	- 0,098 19	- 0,010 38	0,006 571	0,047 8	0,075 359	0,133 373	0,172 027	0,233 749	1,025596
#89	- 0,509 31	- 0,358 41	-0,195  0,152 61	- 0,046 48	- 0,003 335	0,048 86	0,115 627	0,196 98	0,223 469	0,289 617	1,026116	
#90	- 0,505 8	- 0,384 56	- 0,184 47	- 0,139 14	- 0,056 71	0,004 981	0,045 174	0,106 836	0,204 314	0,218 394	0,296 16	1,018734
#91	- 0,966 31	- 0,215 72	- 0,109 85	- 0,061 27	0,020 095	0,042 44	0,044 939	0,063 414	0,080 804	0,114 446	0,162 374	3,681372 938
#92	- 0,885 38	- 0,243 14	- 0,144 23	- 0,085 85	0,003 346	0,040 51	0,067 96	0,082 049	0,090 024	0,137 685	0,262 436	3,742803 172
#93	- 0,923 81	- 0,165 04	- 0,049 49	- 0,030 57	0,013 781	0,043 569	0,063 065	0,080 489	0,097 666	0,112 425	0,189 881	3,517698 573
#94	- 0,866 77	- 0,106 24	- 0,030 44	- 0,008 96	- 0,003 36	0,010 281	0,056 519	0,072 958	0,087 044	0,095 166	0,138 88	3,231367 058
#95	- 0,813 99	- 0,147 02	- 0,073 71	- 0,040 22	- 0,005 75	0,007 332	0,076 969	0,083 594	0,098 638	0,131 991	0,194 95	2,654124 173
#96	- 0,738 12	- 0,241 16	- 0,181 46	- 0,128 54	- 0,081 98	- 0,037 12	0,093 14	0,097 278	0,173 717	0,241 438	0,361 781	1,888063 019
#97	- 0,630 4	- 0,297 88	- 0,235 81	- 0,156 72	- 0,110 24	- 0,060 88	0,082 483	0,109 478	0,175 934	0,339 269	0,414 086	1,525530 941
#98	- 0,169 97	- 0,013 34	- 0,001 52	- 0,000 73	0,000 495	0,002 8	0,007 294	0,007 524	0,007 784	0,009 363	0,018 542	0,219767 084

#99	- 0,797 26	- 0,208 27	- 0,148 34	- 0,072 22	0,006 069	0,045 01	0,053 354	0,055 898	0,095 442	0,227 387	0,257 27	1,249475 633
#100	- 0,755 53	- 0,339 54	- 0,163 66	- 0,128 2	- 0,028 76	0,020 455	0,064 519	0,072 54	0,117 312	0,266 099	0,323 235	1,439307 174
#101	- 0,549 37	- 0,328 21	- 0,152 26	- 0,115 97	- 0,002 91	0,044 612	0,046 114	0,056 966	0,129 572	0,197 549	0,234 921	1,065866 208
#102	- 0,441 71	- 0,324 6	- 0,111 79	- 0,082 84	- 0,009 48	0,033 648	0,042 766	0,061 418	0,084 651	0,135 476	0,213 533	0,856934 616
#103	- 0,379 17	- 0,345 26	- 0,128 22	- 0,105 47	0,000 143	0,029 068	0,047 786	0,060 314	0,079 092	0,169 471	0,217 022	0,778667 674
#104	- 0,404 75	- 0,213 06	- 0,018 01	- 0,005 1	- 0,003 52	0,000 379	0,002 155	0,009 72	0,026 957	0,067 608	0,137 163	0,693805 541
#105	- 0,465 47	- 0,222 53	- 0,120 19	- 0,022 14	- 0,018 13	0,016 0,000	0,028 616	0,051 596	0,083 005	0,221 157	0,826201 988	0,826201 103
#106	- 0,452 33	- 0,328 03	- 0,154 5	- 0,097 04	- 0,070 38	0,017 975	0,038 109	0,073 656	0,139 594	0,157 12	0,271 823	0,862687 31
#107	- 0,444 9	- 0,397 56	- -0,128	- 0,095 83	- 0,038 5	0,010 261	0,038 185	0,086 116	0,143 616	0,156 695	0,272 556	0,849898 137
#108	- 0,495 11	- 0,406 99	- 0,155 31	- 0,140 45	- 0,064 5	0,010 347	0,048 401	0,108 372	0,187 65	0,208 717	0,295 951	0,962333 967
#109	- 0,492 91	- 0,334 35	- 0,186 5	- 0,168 8	- 0,089 89	0,015 01	0,047 315	0,103 023	0,213 849	0,244 592	0,257 701	0,970822 686
#110	- 0,453 6	- 0,322 85	- 0,118 99	- 0,103 22	- 0,051 05	0,011 244	0,032 601	0,066 965	0,130 283	0,171 506	0,196 54	0,972793 589
#111	- 0,448 2	- 0,355 41	- 0,155 52	- 0,151 63	- 0,019 75	0,030 089	0,043 136	0,071 213	0,103 488	0,211 292	0,239 651	1,023596 165
#112	- 0,501 96	- 0,330 66	- 0,113 07	- 0,107 7	- 0,000 89	0,028 995	0,045 53	0,066 949	0,113 849	0,154 03	0,190 404	1,022355 142
#113	- 0,590 35	- 0,291 49	- 0,205 03	- 0,171 23	- 0,033 56	0,006 673	0,055 285	0,066 129	0,152 689	0,289 381	0,302 014	1,201219 257
#114	- 0,632 04	- 0,351 07	- 0,217 67	- 0,168 12	- 0,024 51	0,014 692	0,065 313	0,084 688	0,134 794	0,276 854	0,309 45	1,391106 695

#115	- 0,752 03	- 0,195 06	- 0,165 65	- 0,142 06	- 0,039 91	0,002 396	0,070 107	0,071 97	0,174 271	0,202 993	0,287 937	1,458043 793
#116	- 0,691 24	- 0,208 24	- 0,102 49	- 0,069 01	- 0,016 63	0,021 936	0,052 84	0,064 195	0,115 48	0,190 756	0,239 292	1,814224 469
#117	- 0,853 59	- 0,269 04	- 0,089 87	- 0,040 92	- 0,003 79	0,040 71	0,062 737	0,063 655	0,074 886	0,106 239	0,286 56	1,928323 844
#118	- 0,922 74	- 0,282 09	- 0,157 77	- 0,060 7	0,038 105	0,045 912	0,068 2	0,077 295	0,131 92	0,199 818	0,233 502	3,936580 736
#119	- 0,309 59	- 0,088 82	- 0,002 14	- 0,001 49	0,003 463	0,014 294	0,019 281	0,021 917	0,024 944	0,036 036	0,063 58	0,470347 655
#120	- 0,412 2	- 0,102 74	- 0,015 82	- 0,005 75	0,008 476	0,019 811	0,027 869	0,030 264	0,035 548	0,045 125	0,077 989	0,673812 514
#121	- 0,442 44	- 0,133 66	- 0,054 64	- 0,046 11	- 0,006 23	0,029 949	0,030 667	0,033 586	0,045 948	0,095 542	0,132 085	0,774791 432
#122	- 1,036 11	- 0,196 78	- 0,106 55	- 0,072 22	- 0,022 12	0,009 94	0,072 714	0,076 744	0,118 933	0,152 406	0,333 603	2,149229 873
#123	- 0,774 39	- 0,196 71	- 0,181 54	- 0,117 3	- 0,023 43	0,012 663	0,066 877	0,071 107	0,144 099	0,225 656	0,313 45	1,461556 969
#124	- 0,650 61	- 0,262 72	- 0,228 88	- 0,178 2	- 0,036 37	- 0,004 08	0,065 879	0,074 923	0,157 895	0,290 223	0,326 775	1,354461 523
#125	- 0,612 75	- 0,301 8	- 0,157 2	- 0,148 75	- 0,011 62	0,015 255	0,059 498	0,082 36	0,126 37	0,211 887	0,223 046	1,265763 296
#126	- 0,486 35	- 0,318 59	- 0,110 96	- 0,093 18	- 0,007 89	0,030 74	0,043 531	0,064 644	0,101 271	0,135 748	0,189 54	0,984600 395
#127	- 0,408 26	- 0,362 05	- 0,066 38	- 0,029 02	- 0,000 48	0,006 197	0,031 054	0,039 744	0,080 986	0,094 317	0,153 775	0,913388 055
#128	- 0,462 16	- 0,319 93	- 0,162 63	- 0,143 67	- 0,081 02	0,019 114	0,043 498	0,082 421	0,175 376	0,197 203	0,241 669	0,972816 9
#129	- 0,452 32	- 0,375 97	- 0,124 63	- 0,085 47	- 0,042 86	0,013 938	0,030 067	0,072 217	0,122 883	0,147 507	0,277 642	0,868472 156
#130	- 0,450 22	- 0,311 61	- 0,133 99	- 0,072 1	- 0,032 14	0,006 476	0,022 025	0,052 001	0,098 402	0,128 17	0,256 704	0,863365 203

#131	-	-	-	-	-	0,044	0,065	0,079	0,101	0,220	0,258	1,536032
	0,783	0,296	0,183	0,134	0,005	389	666	65	693	504	538	
36	02	68	07	44								
#132	-	-	-	-	0,000	0,003	0,007	0,008	0,008	0,011	0,021	0,256281
	0,196	0,017	0,002	0,001	791	889	905	211	551	364	979	344
07	14	49	17									
#133	-	-	-	-	-	0,005	0,013	0,032	0,066	0,083	0,275	0,798940
	0,421	0,360	0,080	0,033	0,014	223	727	826	006	248	899	161
73	5	18	52	24								
#134	-	-	-	-	-	0,047	0,098	0,160	0,312	0,357	1,467604	
	0,565	0,347	0,242	0,196	0,111	0,024	589	886	505	226	953	
77	91	21	84	52	09							
#135	-	-	-	-	-	0,003	0,055	0,099	0,168	0,235	0,273	1,070774
	0,510	0,325	0,199	0,175	0,014	499	31	348	509	637	706	
31	04	12	67	65								
#136	-	-	-	-	-	0,003	0,042	0,086	0,167	0,196	0,261	1,026218
	0,512	0,353	0,167	0,108	0,036	712	802	494	174	208	011	
6	55	79	38	44								
#137	-	-	-	-	-	0,045	0,113	0,203	0,213	0,296	1,03559	
	0,512	0,382	0,178	0,135	0,059	0,002	577	689	555	314	793	
16	26	25	75	69	12							

Annex 5: < MATLAB code for making the flow regime map out with the result coming from the flow pattern recognition algorithm. This code is saved as

FlowRegimeMapping.m >

```
clc;
clear all;
%%%% Graph for the measurements taken
%% Get data out the excel file
Measurements =
xlsread('Flow_regime_identification.xlsx','horizontal_pipe');
%% Mapping All Measurements
Water = Measurements(1:end,1);
Air = Measurements(1:end,2);
figure
scatter(Air,Water);
grid on
set(gca,'xscale','log');
set(gca,'yscale','log');
title('Measurements taken with Multiphase flow rig Air & Water Straight Pipe');
xlabel('Air Flow Rate [kg/min]'); % x-axis label
ylabel('Water Flow Rate [kg/min]') % y-axis label
axis([0.05 5 1 200]);
%% Mapping with FP results
figure
Intermittent = Measurements(1:end,4);
Annular = Measurements(1:end,5);
StratWavy = Measurements(1:end,6);
SuccessorFail = Measurements(1:end,7);
Flow_rates=Measurements(1:end,1:2);
for i_index=1:length(Flow_rates)
selectedRow = i_index;
if Intermittent(selectedRow,1) == 1;
    scatter(Flow_rates(selectedRow,2),Flow_rates(selectedRow,1), '^', 'b', 'filled')
elseif Annular(selectedRow,1) ~= 0;
    scatter(Flow_rates(selectedRow,2),Flow_rates(selectedRow,1), 40,Annular(selectedRow,1), 'filled', 'o')
elseif StratWavy(selectedRow,1) == 1;
    scatter(Flow_rates(selectedRow,2),Flow_rates(selectedRow,1), 's', 'g')
end
hold on
if SuccessorFail(selectedRow,1) == 1;
    scatter(Flow_rates(selectedRow,2),Flow_rates(selectedRow,1), 80, 'o', 'r')
end
hold on
end
%%%%%%% Make up of the plot
grid on
set(gca,'xscale','log');
set(gca,'yscale','log');
title('Flow Regime Map 56mm Air & Water Straight Pipe');
xlabel('Air Flow Rate [kg/min]'); % x-axis label
ylabel('Water Flow Rate [kg/min]') % y-axis label
axis([0.05 5 1 200]);
```

```
legend('Intermittent','Annular','StratWavy',  
'Location','eastoutside');
```